Spring 5-17-2013

Fatigue Testing and Data Analysis of Welded Steel Cruciform Joints

Alina Shrestha
ashrest2@uno.edu

Fatigue Testing and Data Analysis of Welded Steel Cruciform Joints

A Thesis

Submitted to the Graduate Faculty of the
University of New Orleans
in partial fulfillment of the
requirements for the degree of

Master of Science
In
Engineering
Naval Architecture & Marine Engineering

by

Alina Shrestha

B.S., University of New Orleans, 2011

May, 2013

Acknowledgements

I would like to acknowledge and express my sincere gratitude to several individuals who helped make this thesis possible by supporting and guiding as well as contributing time out of their busy schedules for the preparation and completion of this study.

First and foremost, my gratitude goes to Dr. Pingsha Dong, for making this research possible. His patience and steadfast encouragement, along with unfailing support as my thesis advisor, are greatly appreciated. Indeed, I would not be able to put together this topic, in absence of his guidance.

Besides my advisor, I will always appreciate the professors in the School of Naval Architecture and Marine Engineering for their untiring effort in encouraging me, and all the students as a whole to pursue academic and professional growth. Also, I would like to thank George Morrissey and Ryan Thiel for being available to help whenever needed.

I would like to acknowledge Mr. Larry DeCan for all of the invaluable help and timely advice that he provided throughout the project to keep it running more smoothly.

My sincere thanks also goes to my fellow coworkers for the stimulating discussions, constructive criticisms, for long working hours before deadlines, and for all the fun we had in the last two years.

Lastly, I would like to thank my family and my friends for believing in me and supporting me in all my endeavors.

Table of Contents

List of Figures

List of Tables

Abstract

In this study, ABS Publication 115, “Guidance on Fatigue Assessment of Offshore Structures” is briefly reviewed. Emphasis is on the S-N curves based fatigue assessment approach of non-tubular joints, and both size and environment effects are also considered. Further, fatigue tests are performed to study the fatigue strength of load-carrying and non-load-carrying steel cruciform joints that represent typical joint types in marine structures. The experimental results are then compared against ABS fatigue assessment methods, based on nominal stress approach, which demonstrates a need for better fatigue evaluation parameter. A good fatigue parameter by definition should be consistent and should correlate the S-N data well. The equivalent structural stress parameter is introduced to investigate the fatigue behavior of welded joints using the traction based structural stress approach on finite element models of specimens, and representing the data as a single Master S-N curve.

Key words: Fatigue, ABS, Size Effect, Master S-N Curve, Equivalent Structural Stress, Traction Stress, Toe Failure, Root Failure

I. Introduction

Background

Fatigue failure in ship and offshore structures is not an unusual sight. The marine structures not only experience the static loads, but also the dynamic loads that exist mainly due to the seaway excitations or wave loads resulting in local changing pressures, the engine excitations that cause elastic vibrations, and varying loads because of loading and unloading conditions. Such dynamic or cyclic loading of various frequencies and amplitudes causes damage in the crystalline structure of the material. The microscopic cracks become visible due to the grain size level plastic deformation; such microcracks then either grow independently or join other microcracks to eventually form macrocracks only to propagate into a main crack and structural failure in the last cycle of the fatigue life.

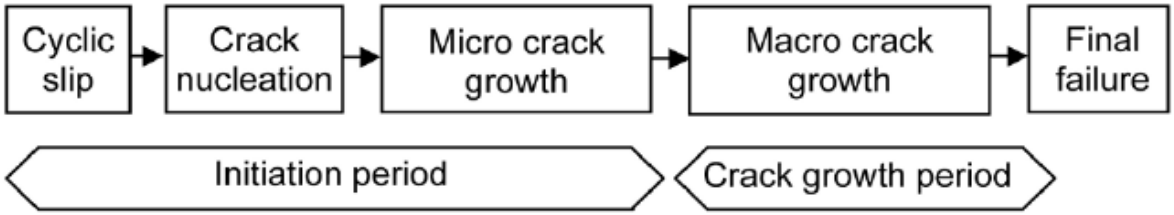

Figure 1 Different phases of the fatigue life

Traditionally, the structures are designed for maximum static loads (or design loads) focusing mainly on the ultimate strength and the buckling strength; however, fatigue strength is one of the major failure modes and thus, is rapidly gaining importance in the structural design of maritime structures and the associated rules.

In extreme cases, fatigue can lead to a total loss of offshore structures or ships resulting in substantial costs each year, and potential loss of life. Such tragedies have occurred throughout the maritime history since there have been several disasters involving fatigue failure of the structures.

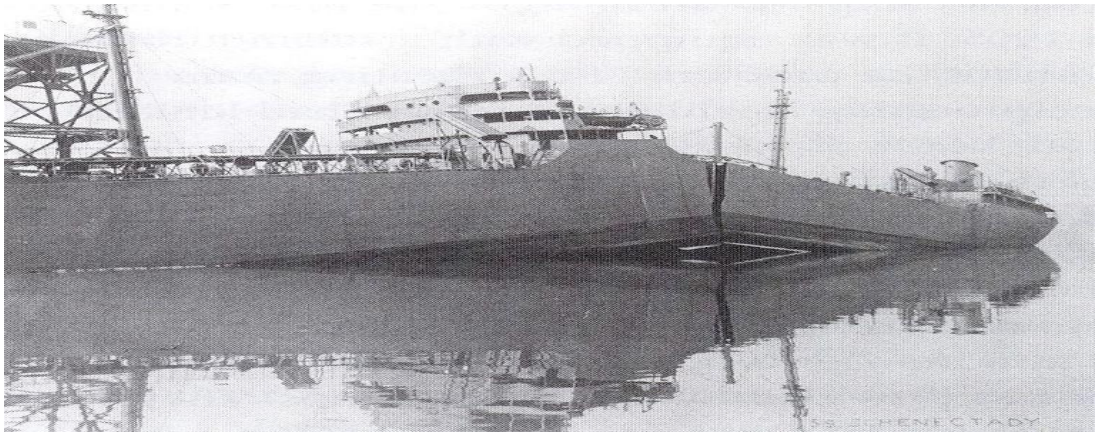

Figure 2 Fatigue failure of S.S. Schenectady, Liberty Ship

Figure 3: (Left) Hull fracture of passenger ship, S.S. America ; (Right) Floating drill platform, Alexander Kielland, capsized after fatigue failure in one cross-brace securing the columns

Historical catastrophes indicate that fatigue strength should be an important consideration while designing structures. Moreover, these days, every effort is made to increase the power-to-weight ratio of sophisticated maritime structures, which increases the vibrational problems, reduces the actual structural material, and thus, results in the reduction of the fatigue strength margin. High-tensile steel is introduced to meet the demand of reduced structural weight, which normally indicates heightened static strength, but similar fatigue strength as of mild steel.

High possibility of fatigue failures occur particularly in the welded structures because of the poor fatigue performance of many welded joints. Welding introduces inhomogeneity in material since additional filler material is utilized implementing subsequent heating and cooling process. Weld includes all kinds of defects like inclusions, pores, undercuts etc, and the shape of weld profiles presents geometric variations thus causing high stress concentrations. Furthermore, welding results in the residual stresses and distortions in the structure, thus severely affecting the fatigue behavior. Clearly, ships and offshore structures consist of various weld joints and thus, this emphasizes the need to consider the potential fatigue failure at the design stage early on in any project.

The fatigue strength of a welded component is defined as the stress range ($\Delta\sigma$) that fluctuates at constant amplitude, causing failure of the component after a specified number of cycles (N). The stress range is the difference between the maximum and the minimum stress values, as shown in Figure 4. Similarly, the ratio of minimum to maximum stress values is denoted by R-ratio. The number of cycles to failure is known as the fatigue life of the component.

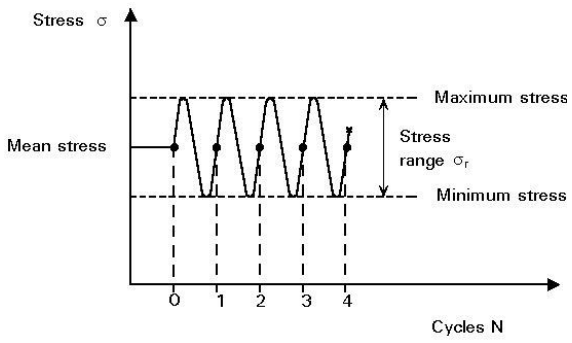

Figure 4: Constant amplitude stress history

Several research efforts are ongoing in order to study the effective fatigue strength evaluation approaches for these welded structures. In addition to that, substantial efforts are made towards the introduction of various standards and fatigue design codes for the marine industry in order to provide an accurate estimate of fatigue life of ships and offshore structures. The codes used by several classification societies are based mainly upon the test data accumulated from fatigue tests on some small-scale specimens integrating the weld detail of interest, by statistical analysis. They also consider the data from actual fatigue damages in ships and other structures. Most rules present a series of S-N curves associated with typical welded joint details, where S is the nominal stress range adjacent to the weld detail and N is the number of cycles corresponding to that stress range. Each S-N curve represents a structural detail based on joint geometry, loading mode, crack location etc.

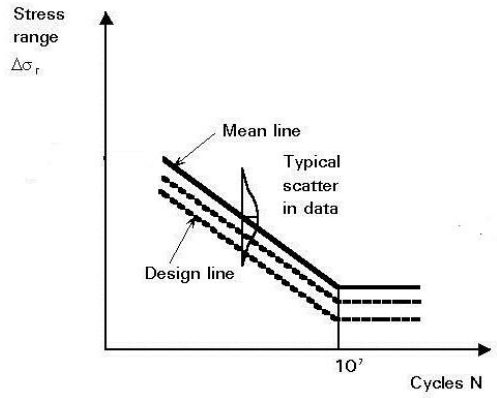

Figure 5: Typical S-N curve for constant amplitude tests

Unlike the fatigue behavior of un-welded structures, the welded joints have unique fatigue features. One of the fundamental differences in fatigue of welded to non-welded structures is that the S-N data of welded joints have a characteristic slope within long-life regime; whereas the latter do not. Similarly, there are no significant effects of applied mean stresses (or R-ratio) on welded joints' S-N data. A number of organizations adopted S-N design curve method in their codes and standards so that the designers can conveniently predict the fatigue life of a certain structural detail by merely using the stress range.

As convenient as it may sound, this is exactly where most of the issues relevant to fatigue lies. There remain two key issues in the fatigue evaluation method, and they are:

i) How to determine stresses?
ii) How to choose an S-N curve?

As mentioned earlier, each S-N curve represents a typical joint type or weld category based on geometry, loading mode as well as crack location. Theoretically, there is infinite number of such S-N curves if the parameters like joint geometry, loading mode, plate thicknesses, and crack locations are considered as a continuous variable over a continuum. Thus, there is often confusion in which S-N curve to select and if the selected curve is correct.

Mathematically, the stress is ill-defined at the locations with sharp notches, and unfortunately, the most fatigue prone locations of welded joints are sharp notched locations or the positions with very small radius such as weld toe or weld root. Several approaches exist in order to accurately estimate stresses at such locations.

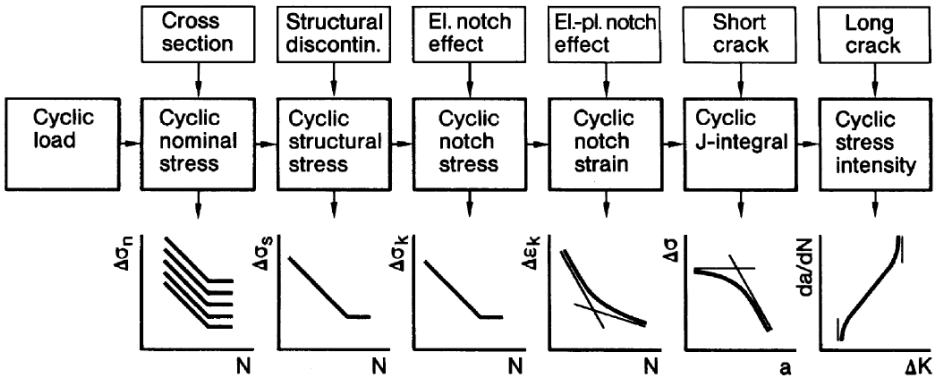

Figure 6: Approaches to describe the fatigue strength

Nominal Stress approach uses the nominal stress range, $\Delta\sigma_n$, which is calculated using internal or external loads and the relevant cross sectional area.

Geometric structural stress or hot-spot stress approach uses the structural stress range, $\Delta\sigma_s$, at the weld. It takes the effect of the structural discontinuity into account.

Notch stress approach and notch intensity approach use the elastic notch stress range, $\Delta\sigma_k$, or the stress intensity, and thus considers the influence of notch effect of the weld toe or root.

Notch strain approach uses the local elastic-plastic strain range, which presents the damage process in the material.

Crack propagation approach uses the J-integral or the stress intensity range, ΔK, and hence determines the crack propagation rate given by da/dN.

Thus, it can be observed that several approaches exist in an effort to precisely find a proper stress value. The former two methods, namely nominal and hot-spot stress methods have been adopted by several classification societies in their design guidelines to estimate the fatigue strength of structures. Recently, Master S-N curve approach based on structural stress method is on the rise. It provides a mesh insensitive method (when Finite Element Analysis is used) to determine stresses at the sharp-notched locations with consistency. The principle of traction based structural stress approach is established on elementary structural mechanics theory.

In addition to the two key issues mentioned above in fatigue evaluation methods, it is important to indicate that a good fatigue parameter should include following properties.

i. Consistency in stress determination
The evaluated stress at any position of the structure should be consistent everywhere and all the time. This calculated stress should not vary or else the calculation goes in vain. Consistency is one of most important properties that a solid fatigue parameter should possess. However, it is certainly not sufficient to be merely consistent; the determined stress has to be correct and the way to validate the accuracy is by data correlation.

ii. Effectiveness in S-N data correlation
When it comes to S-N data, there is quite a bit of scatter in the S-N plot. However, with tremendous amount of collected data, researchers have managed to find a trend to come up with

S-N curves that marine industry has been using worldwide. Each S-N curve has its upper and lower limit based on the scatter of the data. The determined stress that falls into the S-N plot without increasing the scatter band, rather, collapsing the scatter band into fairly narrow band demonstrates strong data correlation, and hence the accuracy of the fatigue parameter. Therefore, a good fatigue parameter should not only possess the effectiveness in S-N data correlation, but also the consistency in stress determination.

Objective

The main objective in this thesis is to review and apply the fatigue design guideline of a major American marine classification society, American Bureau of Shipping, to several loaded and non-loaded steel cruciform joints, and experimentally validate the newly developed master S-N approach in comparison with the ABS guidelines.

II. Literature Review

Introduction

Among several classification societies linked to the marine industry, American Bureau of Shipping (ABS) is one of the major organizations that have been involved in the fatigue technology development. Ship Structure Committee (SSC) has carried out several fatigue research projects with the funding from ABS, in an effort to avoid the critical issue of fatigue fractures in ships and other offshore structures. ABS, in coordination with other professional organizations, classification societies, universities and private industry, has combined the vast knowledge of fatigue behavior of structures from several researches, to create fatigue design criteria for marine structures. This section conducts an extensive review of the main fatigue design rules that are in American Bureau of Shipping, Publication 115, Guide for The Fatigue Assessment of Offshore Structures.

Approach

ABS Guideline contains detail fatigue assessment procedures and significant amount of information regarding fatigue behaviors of welded and un-welded, tubular and non-tubular structures. However, in regards to the objective of this thesis, the fatigue assessment of only plate structures or non-tubular structures is reviewed, and moreover, the document prioritizes the welded plate joints since it is expected for the fatigue cracks to initiate from the joints.

There are two major approaches when conducting the fatigue assessment of any structure.

1) Fracture Mechanics Approach
2) S-N Curve Approach

Although fracture mechanics methods are briefly mentioned in the guidance, this approach is not directly utilized in the industry. It is often used for fatigue analyses as a supplement to the S-N data, or for use in supporting studies that deal with fatigue related issues. When concerned with the acceptable or minimum detectable flaw size or crack growth prediction, fracture mechanics has a significant application. Since the latter approach, i.e. S-N Curve approach dominates the practical application in the industry, ABS employs S-N Approach as the fatigue assessment tool for the determination of the fatigue strength.

Review of ABS Fatigue guideline

The principal objective of this section is to review the main fatigue design rules contained in ABS Publication #115, Guide for the Fatigue Assessment of Offshore Structures. Fatigue assessment, in the Guide, is achieved by the combination of nominal stress ranges, structural hot-spot stresses, relevant S-N curves, and the Palmgren-Miner linear cumulative damage accumulation rule in order to account for the variable stress amplitudes. The failure is recognized when the cumulative fatigue damage goes beyond unity.

The main provision of fatigue design rules in ABS is based on a set of eight (8) fatigue resistance curves. These curves are obtained from test results of a set of constructional details, established from constant amplitude

tests. In addition, the thickness effect as well as the corrosive environment effect is considered, and the fatigue curves are adjusted accordingly.

This approach of classification scheme of the structural details, the S-N curves, and the adjustments made to the curves are mostly derived from DEn(1990) and HSE(1995) criteria. Thus, in the context of fatigue design, ABS Guide can be regarded as a "hybrid" of the above-mentioned criteria.

S-N Curve Approach

After a comprehensive review of fatigue test results and fatigue strength models for welded joints, ABS established a family of S-N curves for marine structures in the ABS Guidance on the Fatigue Assessment of Offshore Structures. The ABS Guide widely employs S-N curve-based approach of fatigue assessment of any structure detail. S-N curve defines the fatigue strength in the stress-based approach to fatigue, and thus can be represented as a table, curve or equation. For design of welded non-tubular structures, the stress determination approach used in the S-N method and the S-N curves are :- nominal stress approach and hotspot stress approach. These approaches will be discussed later below.

Design S-N Curve Definition

The fatigue tests data obtained after constant amplitude fatigue tests when plotted in a log-log space, tend to plot as a straight line, and this is regarded as the mean curve of the S-N data. The mean curve passes through the center of the data through the application of the least squares method.

The linear model thus employed when the S-N data are plotted in a log-log space is given by

$$\log(N) = \log(A) - m\log(S) \quad (1)$$

The empirical constants, A and m are called fatigue strength coefficient and the fatigue strength exponent respectively. S is the independent stress range variable, whereas N is the dependent variable.

The design S-N curve however is defined on the safe (lower) side of the S-N data, or in other words, it is defined as the mean curve minus two standard deviations of log N, which represents 95% survival probability with 75% confidence or better.

Thus the basic S-N curves, which are established from constant amplitude tests, are of the form:

$$\log(N) = \log(A) - m\log(S)$$

When,

$\log(A) = \log(A_1) - 2\sigma$, the above basic S-N Curve signifies the design S-N curves.

N = predicted number of cycles to failure under stress range S
A_1= constant relating to the mean S-N curve
σ = standard deviation of log N
m = negative reciprocal slope (or simply, slope) of the S-N curve

From several welded joints fatigue data, the parameter 'm,' slope is approximately equal to 3.0 which is similar to the slope of the Paris fatigue crack growth law ($da/dN = C(\Delta K)^n$), which for most materials is n = 3. Therefore, in ABS guide, a fixed value of 'm' equal to 3.0 is assumed, and the method of least squares is used to estimate A_1 and σ.

Table 1 below provides the parameters for ABS "In-Air" S-N curves.

Table 1: Details of the Basic "In-Air" S-N Curves

Class	A_1	A_1		m	Standard Deviation		A
		$\log_{10}$	$\log_e$		$\log_{10}$	$\log_e$	
B	2.343×10^{15}	15.3697	35.3900	4.0	0.1821	0.4194	1.01×10^{15}
C	1.082×10^{14}	14.0342	32.3153	3.5	0.2041	0.4700	4.23×10^{13}
D	3.988×10^{12}	12.6007	29.0144	3.0	0.2095	0.4824	1.52×10^{12}
E	3.289×10^{12}	12.5169	28.8216	3.0	0.2509	0.5777	1.04×10^{12}
F	1.726×10^{12}	12.2370	28.1770	3.0	0.2183	0.5027	0.63×10^{12}
F_2	1.231×10^{12}	12.0900	27.8387	3.0	0.2279	0.5248	0.43×10^{12}
G	0.566×10^{12}	11.7525	27.0614	3.0	0.1793	0.4129	0.25×10^{12}
W	0.368×10^{12}	11.5662	26.6324	3.0	0.1846	0.4251	0.16×10^{12}

ABS guideline specifies the knee of the curve at 10^7 cycles for the in-air details. Since the test data are much limited in this range of fatigue cycles, an extrapolation of the S-N curve into this high cycle range involves a change in slope. For in-air structures, the slope beyond 10^7 cycles is:

r = m+2

Thus, if N_Q is the reference number of cycles and S_Q is the corresponding stress range at which the change of the slope occurs, from Figure 7, the relationship between N and S can be written as:

$N = A.S^{-m}$ if $N < N_Q$ (2)

$N = C.S^{-r}$ if $N > N_Q$ (3)

Joint Classification Scheme

A joint classification system helps to relate the description of weld details to their corresponding design S-N curves. There are eight individual S-N curves that denote eight 'nominal' classes that the structural details can be categorized into, namely B, C, D, E, F, F2, G, and W. This classification is based on the geometric arrangement, the direction of loading, and the location and mode of possible fatigue crack. Refer to the Appendix A for the full list of the classification of structural details.

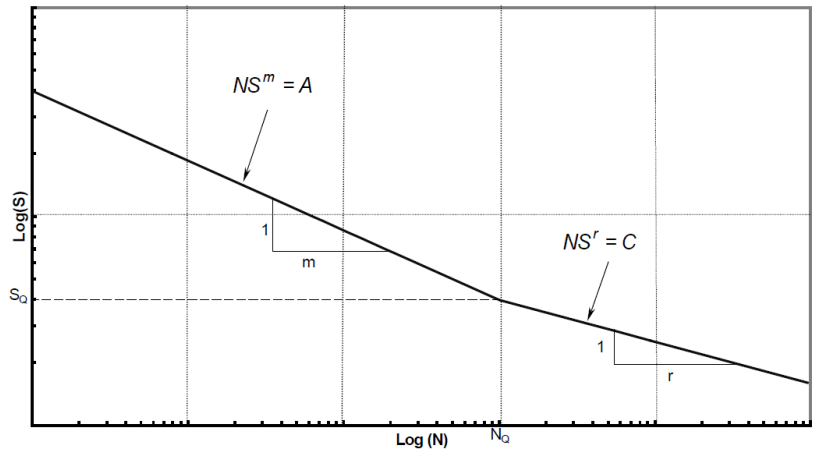

Figure 7: Two-Segment S-N Curve

Adjustment to the S-N Curves

In general, the laboratory specimens that the S-N data are based on are considered different in geometry from the actual size of the structural component. Thus, some adjustments are needed to achieve the expected performance for actual structural details. In this regard, ABS identifies two major considerations that require special awareness and possible adjustment in the fatigue assessment process. These are the effect of thickness and the relative corrosiveness of the environment in which the structural detail is subjected to variable stress.

Scale or Thickness Effect

The fatigue performance of welded joints is dependent on the plate thickness to some extent. For the same stress range, the detail's fatigue strength, which cracks from the weld toe, decreases with the increase in plate thickness. The stress concentration to greater depth in thick sections influence the cracks more than in thin ones, thus the fatigue performance changes with the change in thickness of the structure. The size effect in fatigue in which larger sections tend to be weaker is manifested in welded joint fatigue by a thickness adjustment.

In ABS Guide, the basic design S-N curves are applicable to the structural components having thickness that do not exceed the reference thickness (t_R) of 22 mm. However, the adjustments are made to those with the thickness above 22 mm. The ABS recommended thickness adjustment is based on studies of fatigue test data and the models used by others.

The thickness effect is expressed by an adjustment formula:

$$S_f = S(\frac{t}{t_R})^q \qquad t > t_o \qquad (4)$$

$$S_f = S \qquad t \le t_o \qquad (5)$$

Where,

S_f	allowable stress range
S	allowable stress range from the nominal S-N design curve
t_R	the reference thickness
t_0	thickness above which adjustments should be made
t	actual thickness

A "thickness adjusted" S-N curve can be constructed when $t > t_0$ and is of the form:

$$LogN = LogA - mLog[S(\frac{t}{t_R})^q] \qquad (6)$$

Where,

S	unmodified stress range in the S-N curve
t_R	reference thickness (= 22 mm)
t	plate thickness of the member under assessment
q	thickness exponent factor (= 0.25)

Hence, for plates thicker than 22 mm, ABS introduces the design stress penalty of $(t_{ref}/t)^{0.25}$.

Environmental Condition/Corrosion Effect

Fatigue strength is reduced when the structure operates in a corrosive environment. The ABS recommendations to take into account the influence of corrosion on fatigue strength are based on a review of corrosion effects published in several guidance and other recommended documents in practice relating to marine structures. Crack growth rates increase rapidly when the structures are corroded. To account for the

cathodic protection or the free corrosion conditions of the structures in the sea-water, the parameters for "In-Air" curves are modified, and separate S-N curves are provided.

The parameters as given in the ABS Guidance on the Fatigue Assessment of the Offshore Structures, for the 'In-Air' (A) S-N curve, is given by Table 2.

Table 2: Parameters for ABS-(A) Offshore S-N Curves for Non-Tubular Details In Air

Curve Class	*A*		*m*	*C*		*r*	N_Q	S_Q	
	For MPa Units	*For ksi Units*		*For MPa Units*	*For ksi Units*			*For MPa Units*	*For ksi Units*
B	1.01×10^{15}	4.48×10^{11}	4.0	1.02×10^{19}	9.49×10^{13}	6.0	1.0×10^{7}	100.2	14.5
C	4.23×10^{13}	4.93×10^{10}	3.5	2.59×10^{17}	6.35×10^{12}	5.5	1.0×10^{7}	78.2	11.4
D	1.52×10^{12}	4.65×10^{9}	3.0	4.33×10^{15}	2.79×10^{11}	5.0	1.0×10^{7}	53.4	7.75
E	1.04×10^{12}	3.18×10^{9}	3.0	2.30×10^{15}	1.48×10^{11}	5.0	1.0×10^{7}	47.0	6.83
F	6.30×10^{11}	1.93×10^{9}	3.0	9.97×10^{14}	6.42×10^{10}	5.0	1.0×10^{7}	39.8	5.78
F2	4.30×10^{11}	1.31×10^{9}	3.0	5.28×10^{14}	3.40×10^{10}	5.0	1.0×10^{7}	35.0	5.08
G	2.50×10^{11}	7.64×10^{8}	3.0	2.14×10^{14}	1.38×10^{10}	5.0	1.0×10^{7}	29.2	4.24
W	1.60×10^{11}	4.89×10^{8}	3.0	1.02×10^{14}	6.54×10^{9}	5.0	1.0×10^{7}	25.2	3.66

The design S-N curves for non-tubular details associated with the parameters in Table 2 are represented by Figure 8. Similarly, the parameters for ABS Offshore S-N Curves associated with the structures in seawater with cathodic protection and free corrosion are given by Table 3 and Table 4 respectively. Each table is followed by the relevant ABS Offshore design S-N Curves.

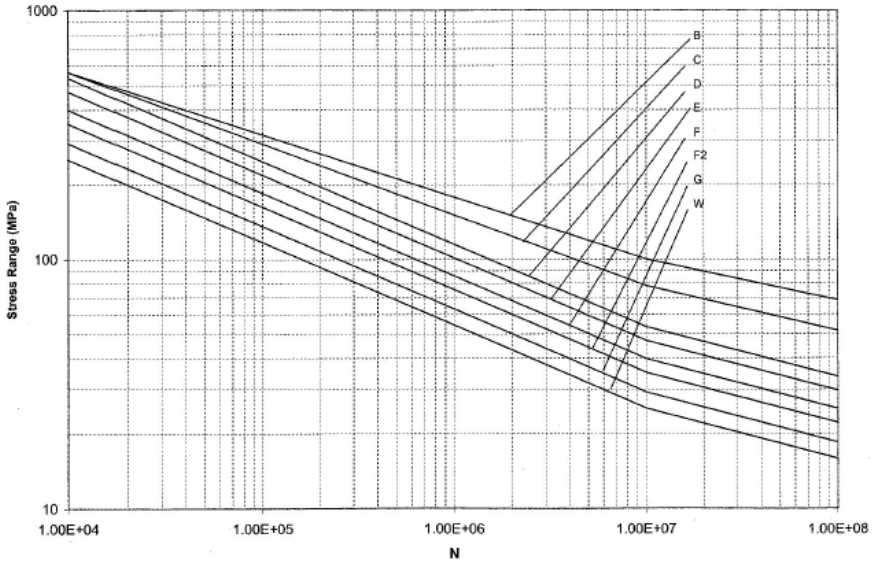

Figure 8: ABS-(A) Offshore S-N Curves for Non-Tubular Details in Air

Table 3: Parameters for ABS-(CP) Offshore S-N Curves for Non-Tubular Details in Seawater with Cathodic Protection

Curve Class	*A*		*m*	*C*		*r*	N_Q	S_Q	
	For MPa Units	*For ksi Units*		*For MPa Units*	*For ksi Units*			*For MPa Units*	*For ksi Units*
B	4.04×10^{14}	1.79×10^{11}	4.0	1.02×10^{19}	9.49×10^{13}	6.0	6.4×10^{5}	158.5	23.0
C	1.69×10^{13}	1.97×10^{10}	3.5	2.59×10^{17}	6.35×10^{12}	5.5	8.1×10^{5}	123.7	17.9
D	6.08×10^{11}	1.86×10^{9}	3.0	4.33×10^{15}	2.79×10^{11}	5.0	1.01×10^{6}	84.4	12.2
E	4.16×10^{11}	1.27×10^{9}	3.0	2.30×10^{15}	1.48×10^{11}	5.0	1.01×10^{6}	74.4	10.8
F	2.52×10^{11}	7.70×10^{8}	3.0	9.97×10^{14}	6.42×10^{10}	5.0	1.01×10^{6}	62.9	9.13
F2	1.72×10^{11}	5.26×10^{8}	3.0	5.28×10^{14}	3.40×10^{10}	5.0	1.01×10^{6}	55.4	8.04
G	1.00×10^{11}	3.06×10^{8}	3.0	2.14×10^{14}	1.38×10^{10}	5.0	1.01×10^{6}	46.2	6.71
W	6.40×10^{10}	1.96×10^{8}	3.0	1.02×10^{14}	6.54×10^{9}	5.0	1.01×10^{6}	39.8	5.78

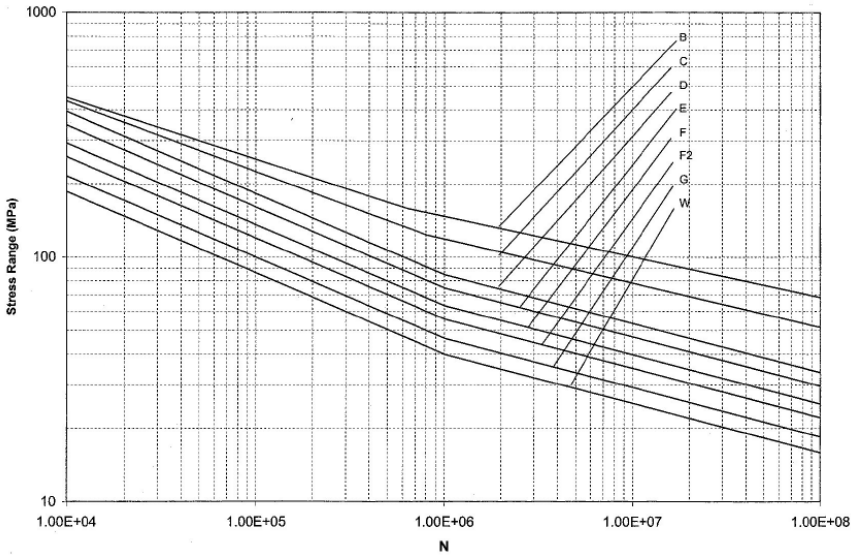

Figure 9: ABS-(CP) Offshore S-N Curves for Non-Tubular Details in Seawater with Cathodic Protection

Table 4: Parameters for ABS-(FC) Offshore S-N Curves for Non-Tubular Details in Seawater for Free Corrosion

Curve Class	*A*		*m*
	For MPa Units	*For ksi Units*	
B	3.37×10^{14}	1.49×10^{11}	4.0
C	1.41×10^{13}	1.64×10^{10}	3.5
D	5.07×10^{11}	1.55×10^{9}	3.0
E	3.47×10^{11}	1.06×10^{9}	3.0
F	2.10×10^{11}	6.42×10^{8}	3.0
F2	1.43×10^{11}	4.38×10^{8}	3.0
G	8.33×10^{10}	2.55×10^{8}	3.0
W	5.33×10^{10}	1.63×10^{8}	3.0

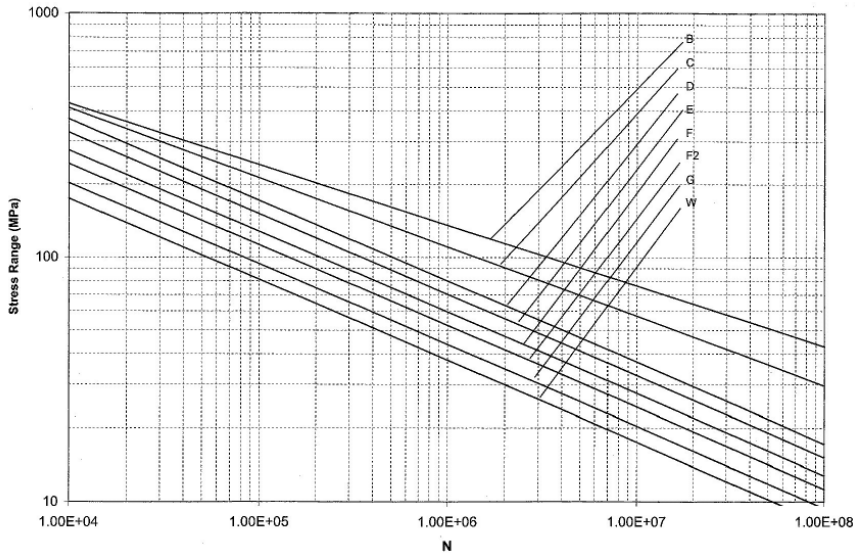

Figure 10: ABS-(FC) Offshore S-N Curves for Non-Tubular Details in Seawater for Free Corrosion

The slope does not change for the the non-tubular structures in seawater for free corrosion.

Design Stresses for Fatigue Assessment

Fatigue assessment of structures is performed with different stresses that are efficient for the considered structural detail. These stresses should be derived in a way that they correspond with the definition of the stresses to be used together with a particular S-N curve.

Nominal Stress

The nominal S-N curves are derived from the fatigue test data, mainly from axial and bending tests. The reference stresses used in the S-N curves are the nominal stresses, typically calculated based on the applied loading and the sectional properties of the specimens. Thus, when using the design S-N curves in a fatigue assessment, the applied reference stresses should correspond to the nominal stresses used in creating these curves. This approach is popular in major industries, however fatigue design based on this approach is cumbersome in terms of securing a series of S-N curves corresponding to each class of joint types and loading modes. In many cases, the loading and geometry of the actual structure are much more complex than the experimental specimen is; hence, it is not always possible to evaluate nominal stresses at each structural component in complex marine structures.

ABS Guide provides following measures for the determination of the appropriate reference stresses required for a fatigue strength assessment:

- In the nominal stress approach, the reference stresses are the local nominal stresses that consider the gross geometric changes of the detail such as cutouts, tapers, haunches, presence of brackets, changes of scantlings, misalignment, etc. It is unnecessary to use a very fine mesh finite element model to determine the required local nominal stresses.
- When assessing the fatigue strength, the stress concentration effect due to the local geometry of the weld must not be taken into account, since the local discontinuity effect is already introduced in the derivation of the S-N curve.

- The principal stress adjacent to the potential crack locations should be utilized if the stress field is more complex than a uniaxial field.

When the fatigue assessment of welded joints is performed, the welded attachment adds uncertainty about the local stress and the applicable S-N curve at the weld locations. These are captured in the nominal stress Joint Classification section. However, when the structure is complicated and too difficult to be classified, the hot spot stress approach is implemented.

Hot-Spot Stress

Hot-Spot Stress approach, or geometric stress approach considers the increase in stress caused by the configuration of the structural detail in consideration. It is applied to extract the stresses at the established hot spot regions or already predicted high stresses areas. For the welded joints, hot spot location is at the weld toe. The stress at the weld toe is calculated by a linear extrapolation of stresses over two reference points in front of the considered weld toe.

Structural or hot-spot stress excludes the local stress concentration due to the weld since the determination procedure of such stress uses the stress at a certain distance away from the weld toe. Hot-spot stresses can be determined by direct measurement of an appropriate physical model, by the use of parametric equations, or through the performance of Finite element analysis (FEA). The use of parametric equations is preferred mainly for the welded tubular joints in the offshore industry. Thus, finite element analysis (FEA) is applied to evaluate the hot-spot stress, according to ABS guidelines. For the linear surface extrapolation of output reference stresses, the reference locations of 0.5t and 1.5t (t - thickness) away from the hot spot to the location of the hot spot are selected. In case of linear shell elements, the components of normal and shear stresses denoted as σ_x, σ_y, and τ_{xy} are individually extrapolated to the hot spot location, and then the extrapolated component stresses are used to compute the maximum principal stress at the weld toe.
In order to obtain a reasonable stress output from Finite Element software, ABS Guide requires appropriate element type and relevant mesh size of the model. Linear elastic quadrilateral plate or shell elements are typically used. The element size around the hot spot should be approximately t x t. The aspect ratio of elements adjacent to hot spot location is required to be 1:1, and the ratio could not exceed 1:3 for the elements away from the hot spot. The corner angles of the quadrilateral shell elements are confined to the range 50 to 130 degrees. The transition from fine mesh to relative coarse mesh should be smooth and uniform.

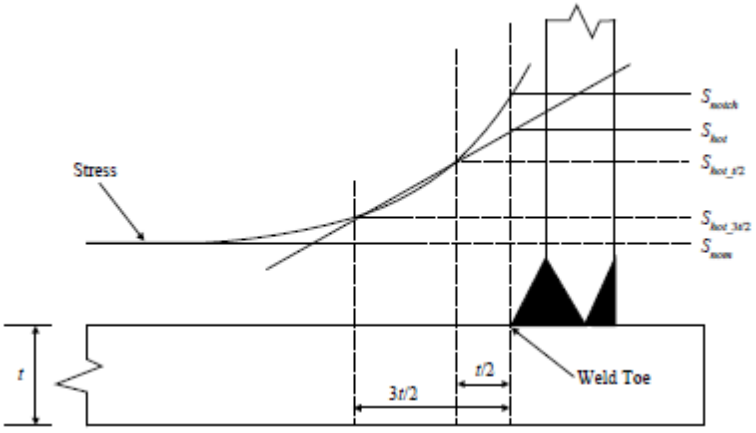

Figure 11: Stress Gradients (Actual & Idealized) Near a Weld

Assessment

Based on the literature review of ABS fatigue guidelines, following conclusion can be derived.

Stress definition is consistent and explicit when the nominal stress based S-N curves are adopted. However, as previously mentioned it is extremely difficult to compute nominal stress for the structures with high level of complexity in geometry as well as loading conditions. Therefore, ABS guideline resolves to the approach like structural hot-spot stress method.

Hot-Spot stress approach reduces the number of eight S-N curves to one S-N curve, which is Class E. Nonetheless, some drawbacks exist when using this approach. The derivation of the hot spot stress requires finite element modeling, and it is sensitive to the element type and the mesh size and shape. There is no clear justification to the reference locations, 0.5t and 1.5t, provided in ABS guide to extrapolate the surface stress.

Also, the adjustment formula to account for thickness effect calls for a specific reference thickness (t_R) along with the thickness exponent, q. The value of reference thickness is equal to 22 mm. The authors supposed that the algorithm for the thickness adjustment formula was obtained using tubular joints, or perhaps using some other procedure. The origin of the algorithm or the procedure to develop the thickness adjustment formula is not well documented, and the reason for selection of the reference thickness is unclear. The value of the thickness exponent provided is 0.25 for all curves. However, it is well known that not all joint types have same effect with the change in thickness. For each class of curve, the rate of change of fatigue lives will vary with the similar change in thickness. Thus, the constant value of this exponent is questionable.

Along with the scale and the environment effect, ABS guidelines is in agreement with the principle that was established well over 30 years ago which concludes that the fatigue strength of the welded structures does not increase with the increase in material strength. The crack propagation rate is not relevant to the material tensile strength, unless the material is exposed to the corrosive environment. Furthermore, it is assumed that a welded structure consist of the residual stress equal to the yield stress. Consequently, the fatigue life is depended on the applied stress range rather than the mean stress, regardless of whether the stress is tensile or compressive.

III. Test Procedures & Results

Introduction

Funded by the National Shipbuilding Research Program (NSRP) in 2011 and building on previous Office of Naval Research (ONR) projects (Huang, et al. 2003 – 07), a joint project "Elimination of Overwelding to Reduce Distortion in Naval Shipbuilding Applications" was initiated. HII-Ingalls and Applied Thermal Science (ATS) fabricated welds to study their behavior through extensive tensile, static shear, fatigue, and dynamic testing at four independent test sites including University of New Orleans (UNO), University of Maine (UMaine), Naval Surface Warfare Center – Carderock Division (NSWCCD), and Concurrent Technologies Corporation (CTC). This section focuses on the steel plate cruciform joints manufactured in order to evaluate the fatigue strength of welded joints. The study provides fatigue test results for load-bearing and non-load-bearing cruciform welded joints in 5 and 10 mm thick plates, which were tested at the University of New Orleans. The test results are then compared to the current ABS fatigue design standards.

Test Method

Test Material

The test specimens were manufactured using 5 mm and 10 mm thick steel plates. They were cut and welded at HII-Ingalls. The steel grades of ABS grade DH36 and HSLA-80 were used for several specimens to be tested; whereas the rest of the specimens were of dissimilar strength, AH36 welded to HSLA-80, in order to reflect weld details in actual ship structures. NSWCCD verified the material property of all base metal plates and the metal weldments. The mechanical properties of these different materials are shown in the table below.

Table 5: Mechanical Properties of the Specimen Material

Material	Yield Strength	Ultimate Tensile Strength	Elongation
AH 36	51000 psi 355 Mpa	71000 – 90000 psi 490 – 620 Mpa	21%
DH 36	51000 psi 355 Mpa	71000 – 90000 psi 490 – 620 Mpa	21%
HSLA 80	36000 – 86000 psi 250 – 590 Mpa	60000 – 95000 psi 414 – 655 Mpa	

Test Specimen

The fatigue specimens varied in material, plate thickness, weld size, and weld method. Another variation was if they were load-bearing (load-carrying) or non-load-bearing (non-load-carrying).

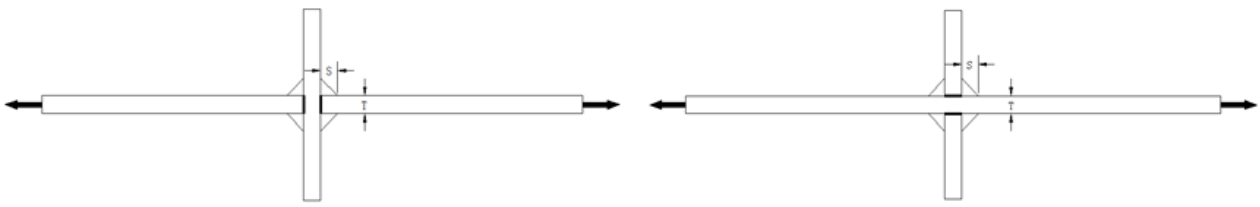

Figure 12: Load-Bearing Cruciform Joint (Left); Non-Load-Bearing Cruciform Joint (Right)

Similarly, the following table shows the number of specimens as well as the variations in the parameters. As can be observed from the table, each load-carrying specimen had a corresponding non-load-carrying cruciform joint with the same parameters. Three individual specimens were fabricated from each plate. Thus, in total, there were 192 cruciform specimens, out of which, 96 were load-carrying and 96 were non-load-carrying specimens.

Table 6: Fatigue Weldment Matrix: Load-bearing (left) and non-load-bearing (right)

Load-Carrying Steel Cruciform Joints					Non-Load-Carrying Steel Cruciform Joints				
Plate No.	Material	Process	Plate thickness [mm]	Weld size [mm]	Plate No.	Material	Process	Plate thickness [mm]	Weld size [mm]
1	DH-36	FCAW	5	3	33	DH-36	FCAW	5	3
2	DH-36	FCAW	5	5	34	DH-36	FCAW	5	5
3	DH-36	FCAW	5	8	35	DH-36	FCAW	5	8
4	DH-36	FCAW	10	5	36	DH-36	FCAW	10	5
5	DH-36	FCAW	10	6	37	DH-36	FCAW	10	6
6	DH-36	FCAW	10	8	38	DH-36	FCAW	10	8
7	DH-36	FCAW	10	10	39	DH-36	FCAW	10	10
8	DH-36	FCAW	10	12	40	DH-36	FCAW	10	12
9	HSLA-80	FCAW	5	3	41	HSLA-80	FCAW	5	3
10	HSLA-80	FCAW	5	5	42	HSLA-80	FCAW	5	5
11	HSLA-80	FCAW	5	8	43	HSLA-80	FCAW	5	8
12	HSLA-80	FCAW	10	5	44	HSLA-80	FCAW	10	5
13	HSLA-80	FCAW	10	6	45	HSLA-80	FCAW	10	6
14	HSLA-80	FCAW	10	8	46	HSLA-80	FCAW	10	8
15	HSLA-80	FCAW	10	10	47	HSLA-80	FCAW	10	10
16	HSLA-80	FCAW	10	12	48	HSLA-80	FCAW	10	12
17	AH36-HSLA-80	FCAW	5	3	49	AH36-HSLA-80	FCAW	5	3
18	AH36-HSLA-80	FCAW	5	5	50	AH36-HSLA-80	FCAW	5	5
19	AH36-HSLA-80	FCAW	5	8	51	AH36-HSLA-80	FCAW	5	8
20	AH36-HSLA-80	FCAW	10	5	52	AH36-HSLA-80	FCAW	10	5
21	AH36-HSLA-80	FCAW	10	6	53	AH36-HSLA-80	FCAW	10	6
22	AH36-HSLA-80	FCAW	10	8	54	AH36-HSLA-80	FCAW	10	8
23	AH36-HSLA-80	FCAW	10	10	55	AH36-HSLA-80	FCAW	10	10
24	AH36-HSLA-80	FCAW	10	12	56	AH36-HSLA-80	FCAW	10	12
25	AH36-HSLA-80	SAW	5	3	57	AH36-HSLA-80	SAW	5	3
26	AH36-HSLA-80	SAW	5	5	58	AH36-HSLA-80	SAW	5	5
27	AH36-HSLA-80	SAW	5	8	59	AH36-HSLA-80	SAW	5	8
28	AH36-HSLA-80	SAW	10	6	60	AH36-HSLA-80	SAW	10	5
29	AH36-HSLA-80	SAW	10	5	61	AH36-HSLA-80	SAW	10	6
30	AH36-HSLA-80	SAW	10	8	62	AH36-HSLA-80	SAW	10	8
31	AH36-HSLA-80	SAW	10	10	63	AH36-HSLA-80	SAW	10	10
32	AH36-HSLA-80	SAW	10	12	64	AH36-HSLA-80	SAW	10	12

FCAW: Flux-Core Arc Welding
SAW: Submerged Arc Welding

Figure 13 displays the basic dimensions of the specimen. The total length of the horizontal base metal was 12 inches, and the vertical attachment was 4 inches long. The specimen was 3 ½ inches wide, into the paper.

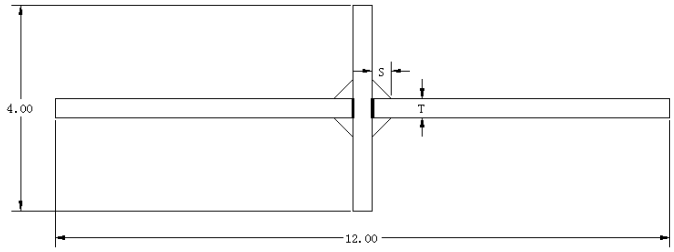

Figure 13: Dimensions of a Cruciform Joint, Weld size (S) and Thickness (T)

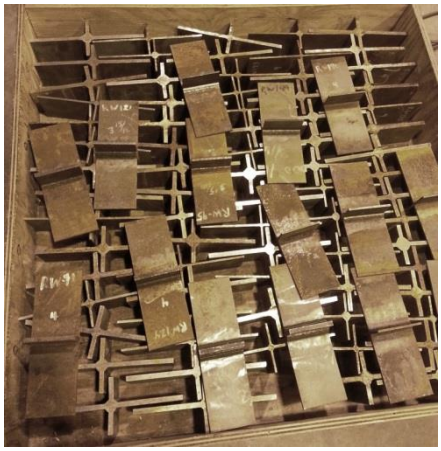

Figure 14: Load-Bearing and Non-Load-Bearing Steel Cruciform Joints received by UNO for Fatigue Testing

Test Machine

Figure 15: MTS Unixial Test Machine at the University of New Orleans

In the laboratory of the University of New Orleans, the fatigue tests were conducted in an MTS uniaxial testing machine where the specimens were loaded using hydraulic grips and cycled axially. The machine has a force capacity of 200 kips and MTS 647 Hydraulic wedge grips with force capacity of 110 kips and maximum operative pressure of 9,000 psi. Hydraulic wedge grips were used to mount the specimens, and to apply the loads on them. Along with the grips, there are four individual (or two pairs of) wedges mounted on the grips. These wedges are 3.5 inches deep, 3.75 inches wide, and opens from 0 to 10.9 mm. The metal brackets are used to keep the specimens aligned in the center of the wedges. The machine operated remotely using FlexTest GT software from which the load levels and frequencies were specified. 5" of gage length was specified for all the 12" specimens to avoid any buckling during the test procedure.

Test Requirements

As per the specification by project sponsor, NSRP, fatigue testing was carried out in accordance with ASTM E466 using gage length of 5 inches.

Load Specification

There were two stress ranges at R = -1 that were applied to the specimens: 30 ksi (+/-15ksi amplitude) and 60 ksi(+/-30 ksi amplitude). The table below specifies the number of specimens tested under the specified loads.

Table 7: Load Specification for Test of Individual Cruciform Joint

	Total Specimens	Fatigue test at stress range 30 ksi [207 MPa]	Fatigue test at stress range 60 ksi [414 MPa]	Spare specimens
Load Carrying	96	32	54	10
Non-load-carrying	96	32	54	10

R ratio = minimum load/maximum load = -1

Distortion Acceptance Criteria

Several test specimens had little to severe misalignments as well as angular distortions. Thus, the Distortion Acceptance Criteria was set for the fatigue test specimens as below:

i. The misalignment/offset in the specimen should be less than or equal to ½ thickness of the through member.
ii. The angular distortion should be less than or equal to ½ thickness of the through member.

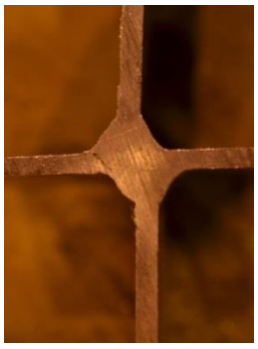

Figure 16: Severe Offset in the Specimen

Failure Criteria

The elevation of cruciform joint's compliance to 100% marked its failure. In other words, the fatigue failure criteria set for all the specimens was at 50% reduction of the specimen stiffness.

Fatigue Failure Mode

There are two major fatigue failure modes: plate failure and weld failure. The former mode of fatigue failure, where the crack initiates for the toe of the weld through the thickness of the base plate is classified as the weld toe failure. Similarly, the latter mode, which initiates from the root of the weld and travels along the weld throat is classified as the weld root failure.

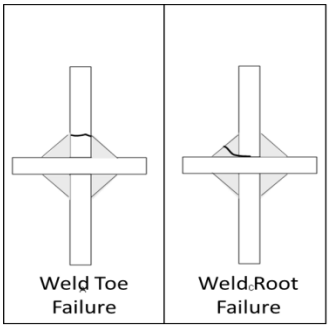

Figure 17: Two Major Fatigue Failure Modes Classification

Test Procedures

Fatigue tests were carried out on all the load-carrying and non-load-carrying steel cruciform joints.

Distortion Check

First, the cross-section of the cruciform specimens were scanned to the computer. Then, using AutoCAD, the misalignment/offset and the angular distortion of the scanned files were measured. The specimens had to fulfill two previously mentioned criteria before considering them fit to test.

If the measurements in AutoCAD displayed that the specimen fulfill both criteria, or if the misalignment and the angular distortion in the specimen were less than or equal to ½ thickness of the through member, then the particular specimen was set aside to test. However, if it failed to fulfill any or both criteria, then it was straightened so that it fulfilled the criteria.

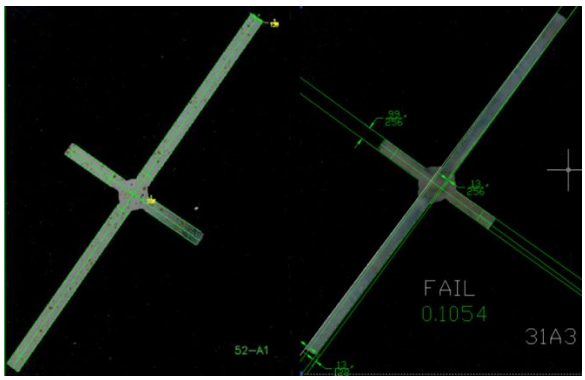

Figure 18: Distortion Criteria Check on the Scanned AUTOCAD Pictures of the Specimens: Pass (Left); Fail (Right)

Distortion Correction

For the specimens that failed to satisfy one or more distortion acceptance criteria, they were corrected or straightened using three point bending die and a hydraulic jack as shown in Figure 19.

Measurements

After making sure that the specimen satisfied both criteria, each weld of the cruciform was marked as weld A, B, C, and D. Then, using Wikiscan, vertical and horizontal weld leg sizes were measured at four different positions of each weld in the specimen. Thus, this resulted in 16 horizontal and 16 vertical weld leg-size measurements for a single specimen.

In addition to the leg size measurements, the actual thickness and the actual width of the specimen was measured to calculate the actual cross-sectional area of the base plate using the digital caliper at different sections of the specimen.

Figure 19: 20 Ton Hydraulic Power Life Bottle Jack

Load Calculation

The applied load was computed based on the desired stress level and the actual cross-sectional area measurements. A specific nominal load level (+/- 15 ksi or +/- 30 ksi) was selected based on the test-matrix provided for the specimen. Then, the actual force amplitude required to maintain that load level was computed as below. The loading was fully reversed and of constant amplitude.

$$Force\ amplitude = Stress\ or\ Load\ level\ \times Cross - Sectional\ Area \quad (7)$$

Mounting of Specimen

Next, the specimen was prepared to be tested on the MTS machine. Several pictures are taken before the specimen was put on the machine as a part of documentation. Then, carefully, gage length of 5 inches was marked. Thus, with 5 inches gage length or the length between the wedges, the specimen was gripped on the MTS machine. The fatigue test machine with a test specimen installed is show in Figure.

Testing & Data Acquisition

Fatigue test of the welded joints were carried out in constant loading mode, which means the specimen was provided with the constant cyclic force (Sine signal). First of all, the force was applied for approximately 100 cycles, to make sure the cruciform was completely gripped and to confirm the initial force and displacement were stable in order to avoid the slippage in the wedges. After verification, the fatigue test was performed. Under the data acquisition part, all the data for first 1000 cycles were stored into the computer hard-drive, then after 1000 cycles, data for 5 cycles in every 100 cycles were stored until the fatigue crack developed in the cruciform and it broke apart completely in two separate pieces. For all the fatigue tests, the applied stress ratio was R = -1, and the cycling frequency for the majority of the specimens were 7 Hertz. For each test, time (sec), axial count (segments), axial displacement (inches), and axial force (kips) were recorded per cycle.

Test Results & Observation

Specimen Pool

Out of the 192 total specimens, only 177 specimens were tested for fatigue. Several specimens did not meet the distortion criteria, and they had to be corrected. However, few of them were severely skewed or distorted beyond repair so they were discarded. Other specimens were retracted from the specimen pool because one of them was destroyed by accident and the data recorded for two specimens were corrupted.

Stiffness Measurement Results

As previously mentioned, load and displacement were recorded per cycle, and then the stiffness curve was derived based on the collected data. The procedure to stiffness calculation is in Appendix B. Figure 20 illustrates load, displacement, and the calculated stiffness curve over the number of cycles (logarithmic) of one of the specimens marked 30-A1, 12 inches long, 3.5 inches wide, and 3/8 inches thick, with the gage length of 5 inches.

In general, a significant reduction in stiffness could be observed for all the specimens right before they fully fractured. The stiffness curve initially remained steady as the test continued and then dropped suddenly as the crack propagated either through thickness of the base plate (weld toe failure) or through the root of the weld (weld root failure). Only couple of hundred of load cycles is then required to break the specimen completely apart when the stiffness of the specimen dropped. This reflects the fact that fatigue crack growth dominates the fatigue lives of the welded joints.

Thickness Effect Results

With respect to the thickness parameter, there were two different thicknesses for the cruciform joint specimens overall. They were the joints with thickness (t) of 5 mm (3/8 inches) and 10 mm (3/16 inches). Several data points were plotted with varying thickness nonetheless keeping all the other parameters constant such as applied load, weld sizes (s), and load-carrying and non-load-carrying joint types in the following plots. There were only different thicknesses; however, from the plots, it can be seen that in general the specimens with thicker base plates (3/8 inches) have lower fatigue lives that the specimens with thinner base plates (3/16 inches).

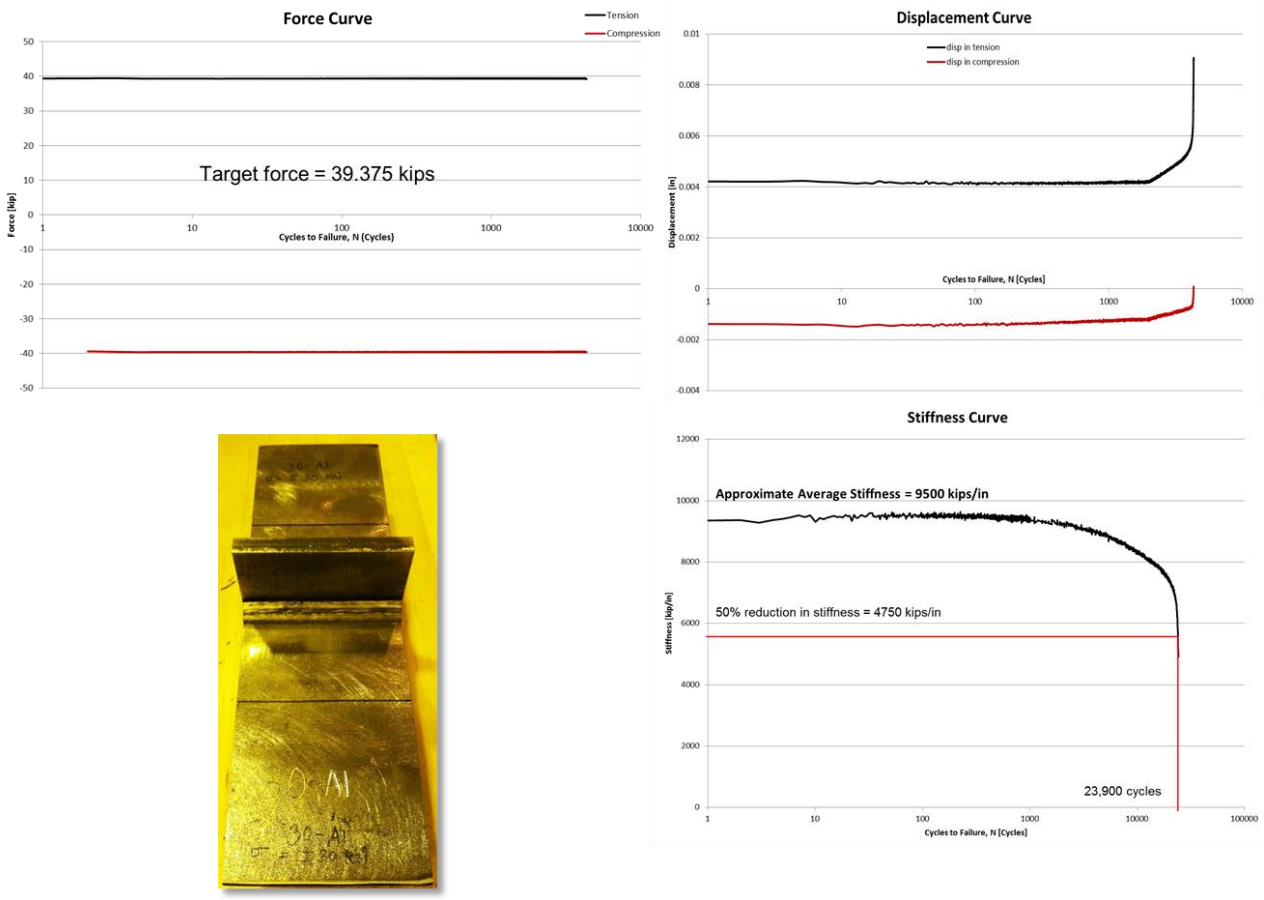

Figure 20: Applied Force over Cycles Plot (Top Left); Displacement over Cycles Plot (Top Right); Specimen 30-A1 (Bottom Left); Stiffness of the Specimen over Cycles Plot (Bottom Right)

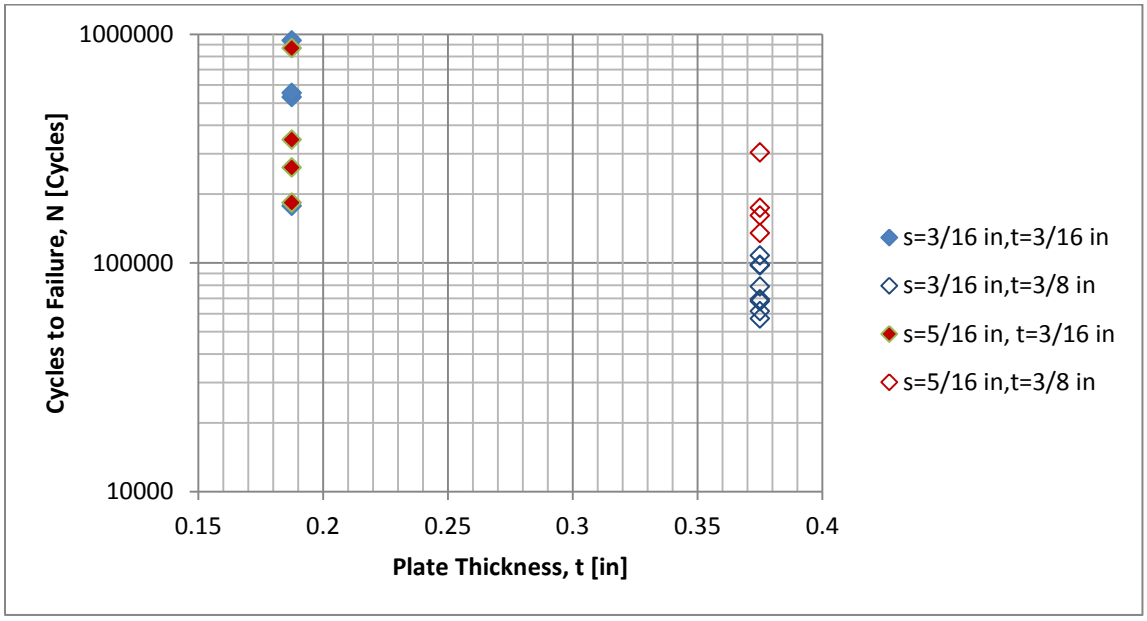

Figure 21: Fatigue Data of Load-Carrying Cruciform Joints with Applied Stress Range of 30 Ksi

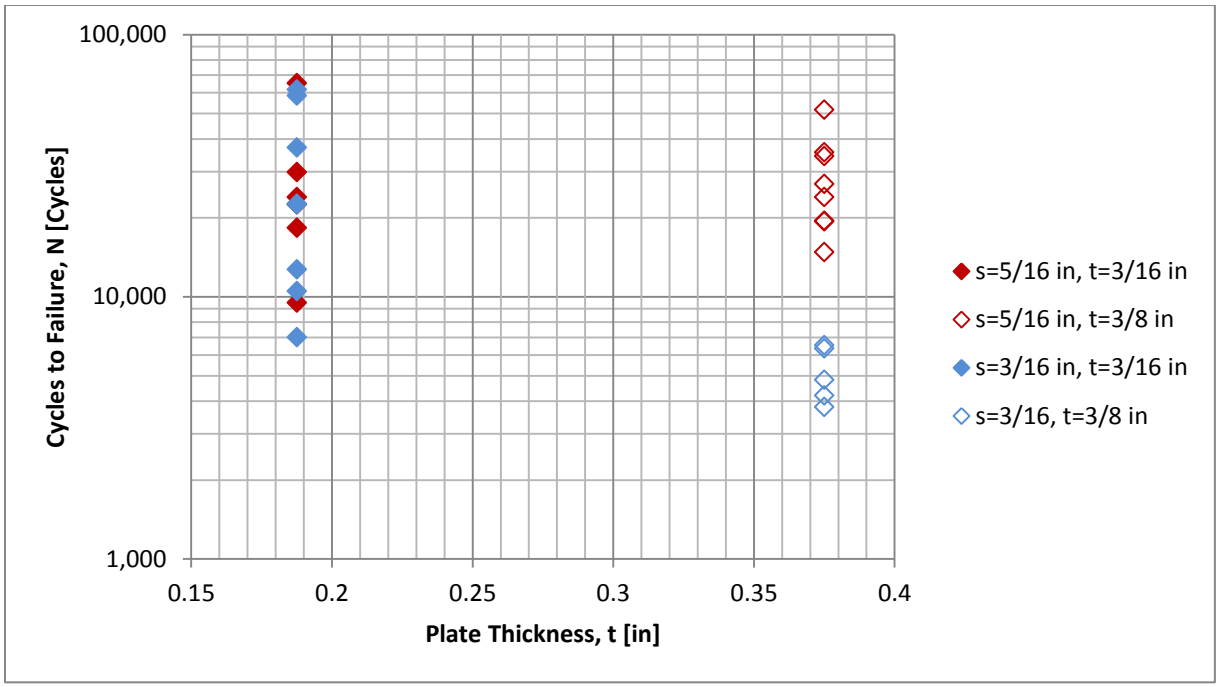

Figure 22: Fatigue Data of Load-Carrying Cruciform Joints with Applied Stress Range of 60 Ksi

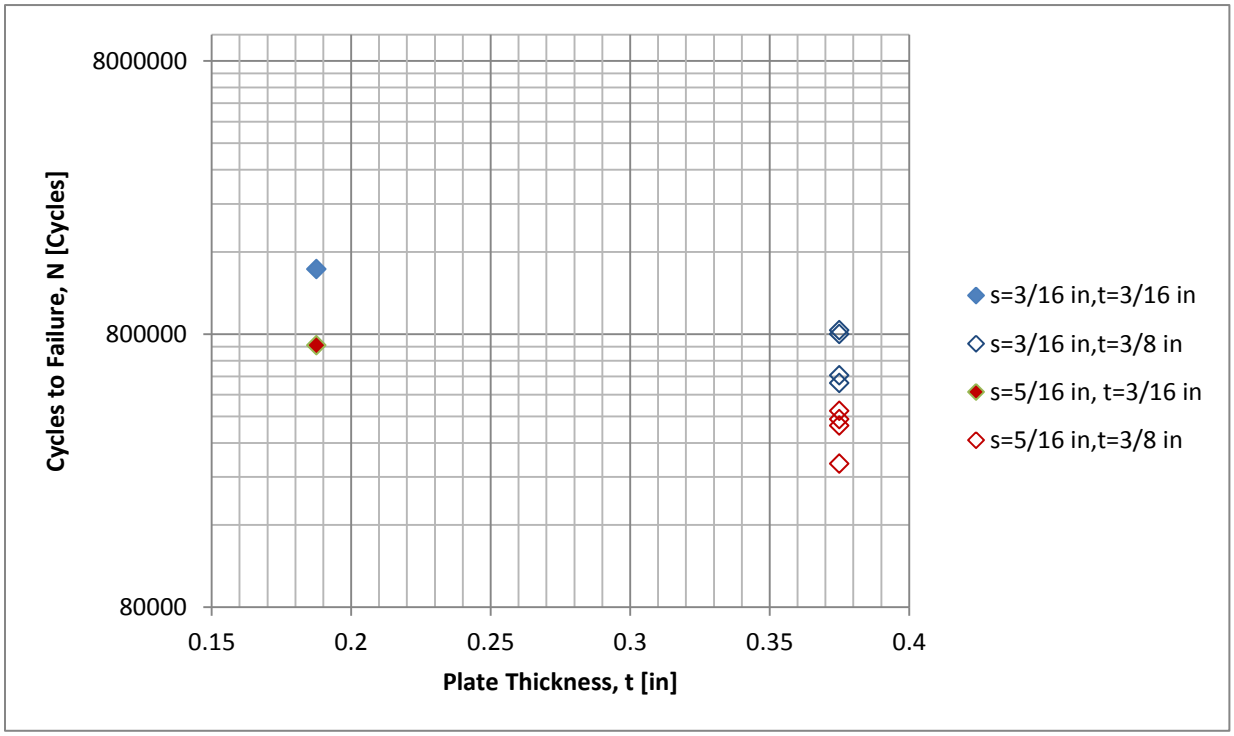

Figure 23: Fatigue Data of Non-Load-Carrying Cruciform Joints with Applied Stress Range of 30 Ksi

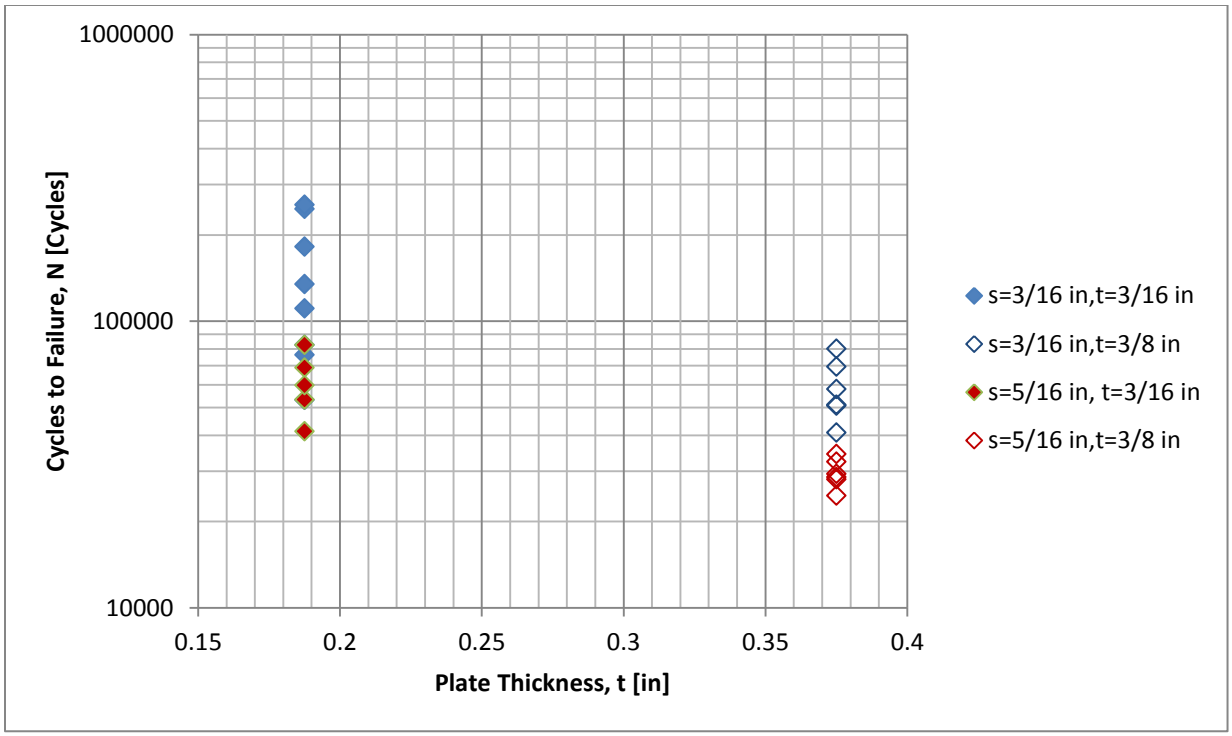

Figure 24: Fatigue Data of Non-Load-Carrying Cruciform Joints with Applied Stress Range of 60 Ksi

Fatigue Failure Path and the Critical Point

The observation of the fracture surfaces after the fatigue tests led to the identification of fatigue failure paths. These failure paths were based on the initiation location of the cracks and their direction of the propagation.

i) Toe failure - The crack started at either side of the weld toe and the crack propagated through thickness of the base metal plate. See Figure 25.

ii) Root failure - The crack initiated at the root of the weld and eventually travelled to the weld surface. See Figure 26.

Besides, few specimens did not develop fatigue crack during the testing, even beyond 2 million cycles, thus, the failure path could not be identified in those joints. Such joints were classified as the runout specimens.

Table 8: Number of Tested Joints and their Fatigue Failure Path

Cruciform Joint Type	Toe Failure	Root Failure	Runouts
Load-bearing	61	30	0
Non-load-bearing	80	0	6

As illustrated in Table 8, none of the non-load-bearing specimens experienced fatigue failure at the weld root; whereas, both load-carrying and non-load-carrying specimens had weld toe failures. Furthermore, only the non-load-carrying specimens had 6 runouts.

Figure 25: Fatigue Failure Path: Weld Toe

Figure 26: Fatigue Failure Path: Weld Root or Weld Throat

In the marine industry standard, despite the inevitableness of fatigue failure, toe failure is usually preferred to the root failures in the welded joints. The toe failures represent the crack in the base metal, which is convenient to locate, and thus, corrective measures can be taken immediately in contrast to the weld root failures where it is not possible to locate the fracture until the complete separation of the joint. Utilizing only non-load-bearing type of structural detail will avoid the weld root failure issue; however, it is not viable at all.

Only for the load-bearing cruciform joints, the fatigue lives when plotted against the corresponding weld sizes (s) normalized by base plate thicknesses (t), a specific marked point can be observed that divides internal weld root failure from the external weld toe failure. Figure 27 shows the cycles to failure of the specimens against the nominal s/t ratio (weld size to the plate thickness ratio) for both stress range levels of 30 ksi and 60 ksi.

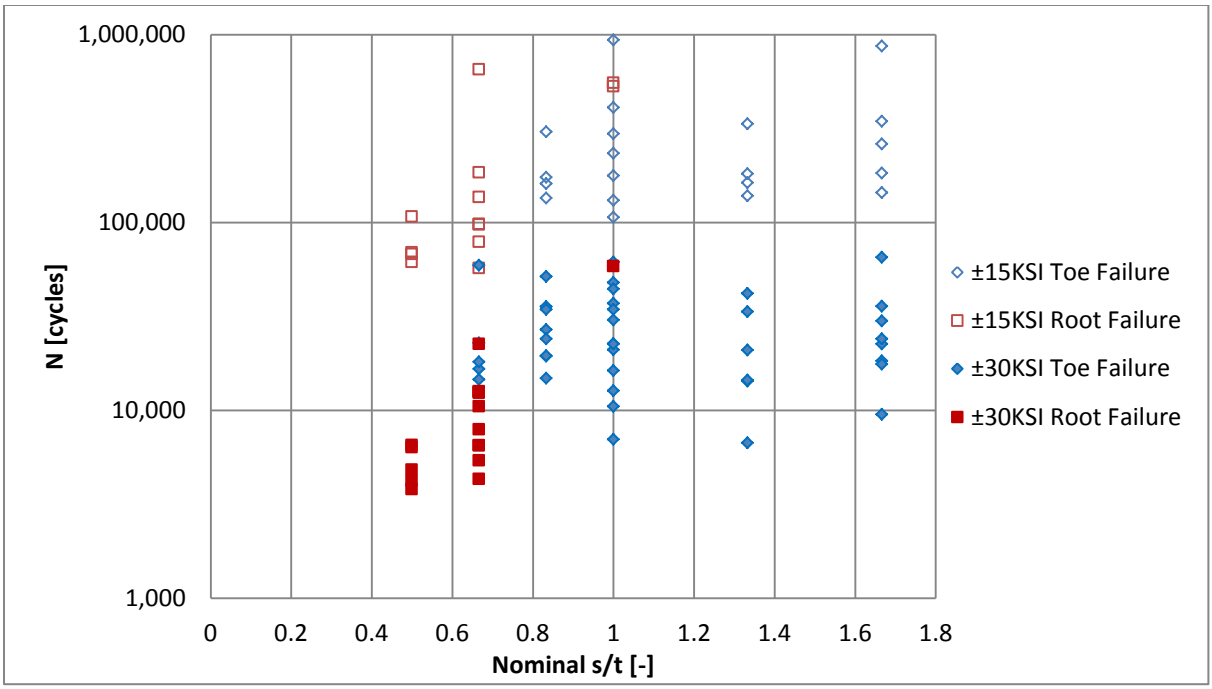

Figure 27: Fatigue Life of Load-Carrying Joints Vs. Nominal s/t ratio, Critical Point

Replacing the nominal weld leg sizes with the actual weld leg sizes and the thicknesses of each specimen, following plot, Figure 28, was generated, which is more justified. The plot clearly confirms that within the s/t ratio region of about 0.75 to 0.95, both fatigue failure modes of weld toe failure and weld root failure exist. However, when s/t ratio of the specimen is below the specified range, the crack occurs at the weld root, and likewise, if s/t ratio of the specimen is beyond this range, the fatigue crack occurs at the weld toe.

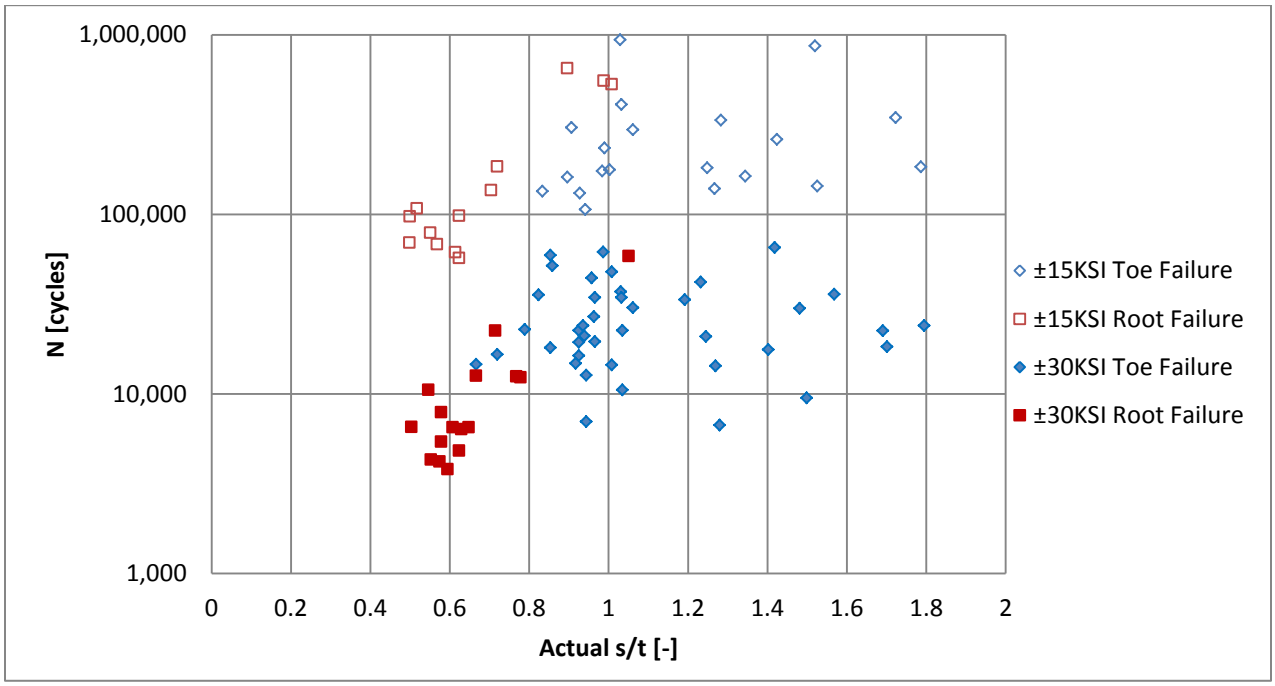

Figure 28: Fatigue Life of Load-Carrying Joints Vs. Actual s/t ratio, Critical Point

Therefore, on the contrary to popular belief that increasing weld size (or overwelding) on any structure prevents the weld root failure, increase in weld size to base plate thickness ratio over $0.75 \leq s/t \leq 0.95$ range would rather confirm weld toe cracking in case of fatigue failure. Additionally, the fatigue cracks that originated from the weld root seemed to have caused a significant reduction in the fatigue strength of the welded joints as compared to the weld toe cracks.

Data Analysis & Discussions

Ultimately, the fatigue test results are utilized to estimate the fatigue life of the load-carrying and non-load-carrying cruciform joints. The fatigue life evaluation of welded structures includes S-N data from actual weldments in order to generate corresponding S-N plots. Thus, using the experimental results from the fatigue test, experimental S-N plots were produced.

As identified previously, there are several uncertainties on how to determine the correct stresses at the weld toe or root locations. Provided the time and scope of this project, only nominal stress approach was utilized in order to generate the experimental S-N plots, and they were compared against ABS design S-N curves from its Publication 115, Guide for The Fatigue Assessment of Offshore Structures.

Statistical Analysis

The correlation of the large database of fatigue test results in order to display a general trend of the data requires a statistic regression analysis. Using the least squares fitting method, the statistical linear regression analysis of the data was performed, and the standard deviation and the R-squared value was computed. Standard deviation shows the variation of the dispersion of data points from the average or mean value of the total data. It is non-dimensional in case of fatigue curves and represent the scatter of log(N), where "N" is the number of cycles. The standard deviation for fatigue method is usually reported as 0.30, 0.40, 0.50, etc. Essentially, well-correlated test data to the mean curve would have low standard deviation. Now, the coefficient of determination or R-squared value provides a quantitative measure of the efficiency of the future outcomes that are predicted by the model. The numerical value of R^2 ranges from 0 to 1; the higher the R^2 value, the better the regression line fits the data set.

The regression model is in the form: $\log(N) = b_0 + b_1 \log(S)$; where N is the number of cycles to fatigue, S is the applied stress, b_0 is the intercept, and b_1 is the inverse slope of the mean regression curve.

Nominal Stress Based Experimental S-N Chart

The load-carrying and non-load-carrying steel cruciform joints were tested with two different nominal stress range levels, 30 ksi and 60 ksi. The S-N charts in the following figures: Figure 29, Figure 30, and Figure 31 exhibit the nominal stress range against the number of cycles to failure for each specimen.

The fatigue test results are presented in terms of nominal stress ranges. The solid lines in the plots are the mean regression line to display the general trend of the data. The mean regression line represents the 50% survival probability. The broken lines are the upper bound and the lower bound curves. The lower bound line is calculated by subtracting two standard deviations of log N from solid line representing 95% survival probability, whereas the upper bound line is calculated by adding two standard deviations of log N from the solid line representing 5% survival probability.

In addition, the standard deviation (σ), R^2 value, and the inverse slope of the plots (b_1) are provided.

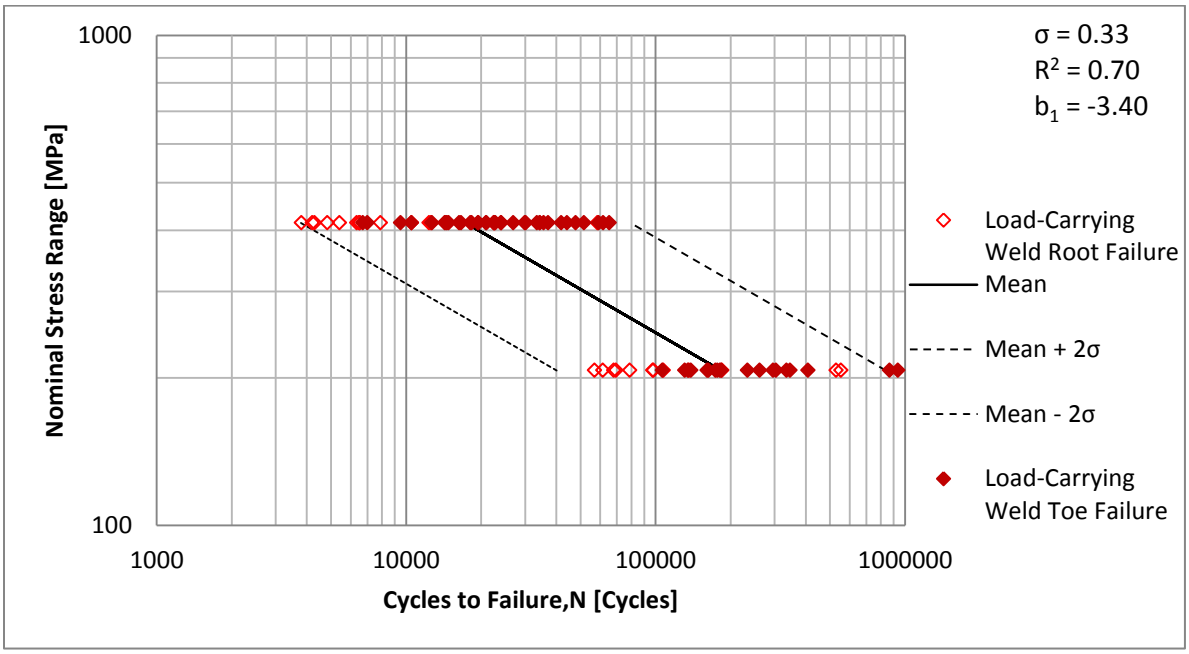

Figure 29: S-N Chart based on Nominal Stress Approach for Load-Carrying Steel Cruciform Joints

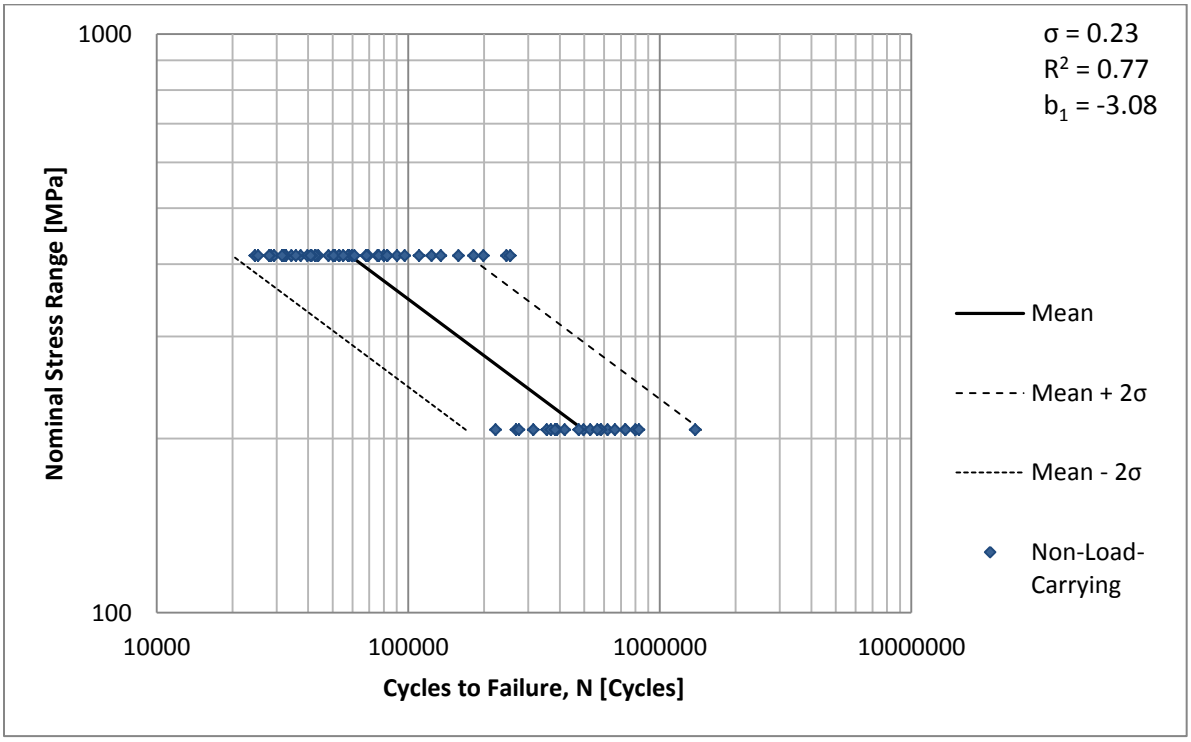

Figure 30: S-N Chart based on Nominal Stress Approach for Non-Load-Carrying Steel Cruciform Joints

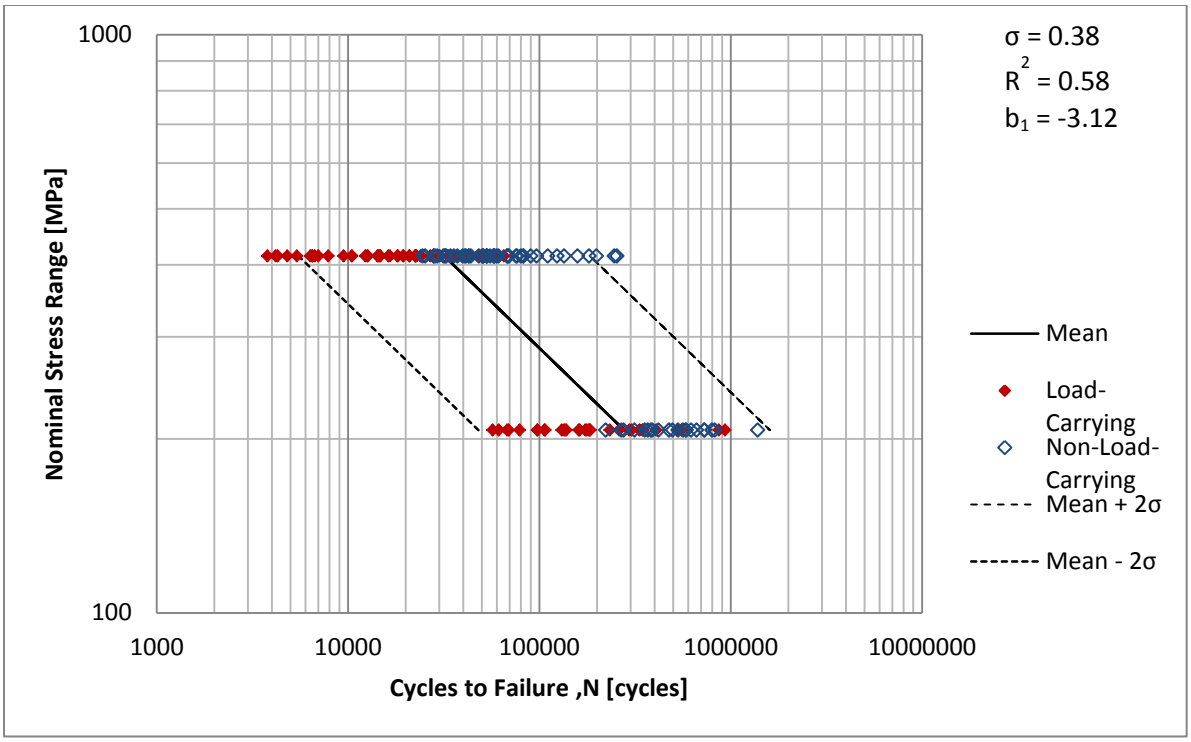

Figure 31: S-N Chart based on Nominal Stress Approach for all Steel Cruciform Joints

The S-N Chart above display a significant scatter in data. The scatter bands, from lower bound to the upper bound, are substantially wide for not only load-carrying and non-load-carrying specimens' fatigue data individually, as in Figure 29 and Figure 30, but also, when combined as in Figure 31. R^2 value for Figure 29 and Figure 30 are 0.7 and 0.77, and the standard deviations are 0.33 and 0.23 respectively. Despite the simplicity in determining the nominal stress, its ability to effectively correlate the fatigue test data is hence certainly questionable with such large scatter bands presented in the plots above. Therefore, when considering nominal stress as a fatigue parameter, it is definitely consistent; however, as demonstrated by the analysis, it does not effectively correlate the S-N data. The least correlation exists when the load-carrying and non-load-carrying specimens fatigue data are put together in an S-N plot based on nominal stress approach.

Comparison of Nominal Stress Based Experimental S-N Curve with ABS Nominal Stress Based Design S-N Curve

Classification of Joint type

In order to compare the experimental S-N curves with the design S-N curves established by ABS guideline, there is a need to classify the load-carrying and non-load-carrying steel cruciform joints into one of the several classes of ABS welded joint types. Based on the geometric arrangement, the direction of loading, and the location and mode of possible fatigue crack, there are three classes that most closely match the testing conditions of the cruciform. Referring to Appendix A, from ABS guidelines:

I. Class F curve represents the non-load-carrying cruciform joints

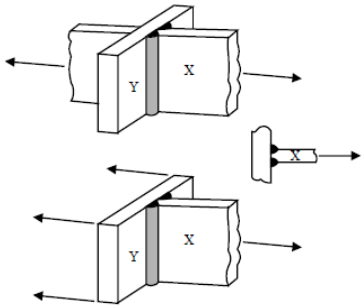

Figure 32: Class F Joint Type from ABS Fatigue Design Guidelines

"Joint made with full penetration welds and with any undercutting at the corners of the member dressed out by local grinding. Member Y can be regarded as one with a non-load-carrying weld."

II. Class F2 curve represents the load-carrying cruciform joints with weld toe failure

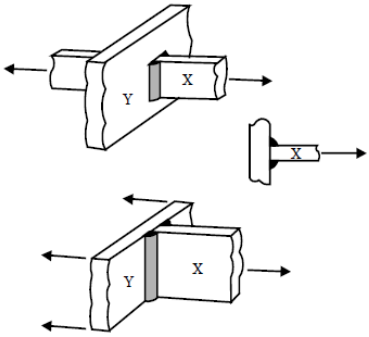

Figure 33 Class F2 Joint Type from ABS Fatigue Design Guidelines

"Joint made with partial penetration or fillet welds with any undercutting at the corners of the the member dressed out by local grinding."

III. Class W curve represents the load-carrying cruciform joints with weld root failure

"In this type of joint, failure is likely to occur in the weld throat unless the weld is made sufficiently large."

"Weld metal in load-carrying joints made with fillet or partial penetration welds, with the welds either transverse or parallel to the direction of applied stress (based on nominal shear stress on the minimum weld throat area)."

Design S-N Curves and Comparison

As discussed in the Literature Review chapter, the design S-N curves in accordance with the ABS guidelines is given by,

$$\log(N) = \log(A) - m\log(S)$$

When,

$$\log(A) = \log(A_1) - 2\sigma$$

Two major adjustments to the S-N curves were considered: Scale or thickness effect and environmental effect. The environmental condition selected for the S-N curve was "In-Air" since all the fatigue tests were conducted in the laboratory. No thickness penalty was applied to any joints for all the tested specimens were thinner than the reference thickness (t_R) of 22 mm. So, the relevant design S-N curves were identified for curve class F, F2, and W, and thus, they were plotted against the experimental S-N data as shown in the figures below.

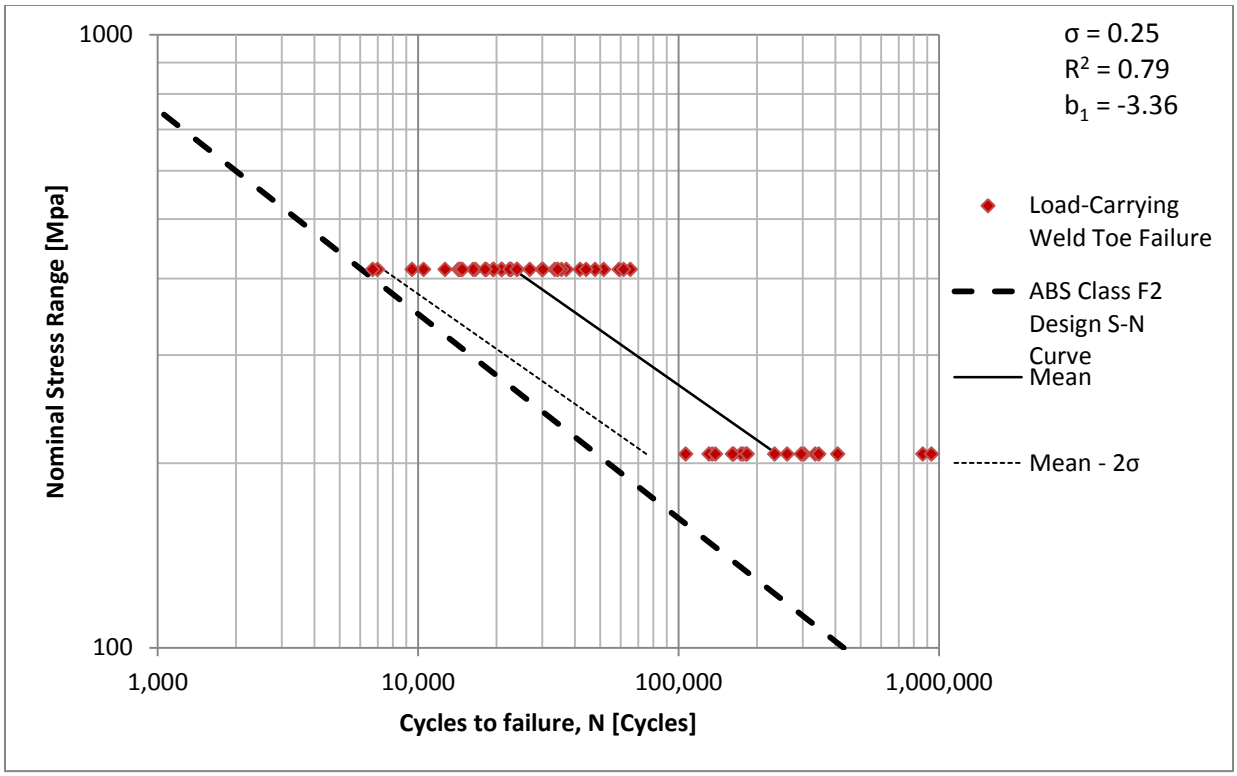

Figure 34: ABS Class F2 Design S-N Curve Vs. Experimental S-N Data of Load-Bearing Cruciform Joints with Weld Toe Failure

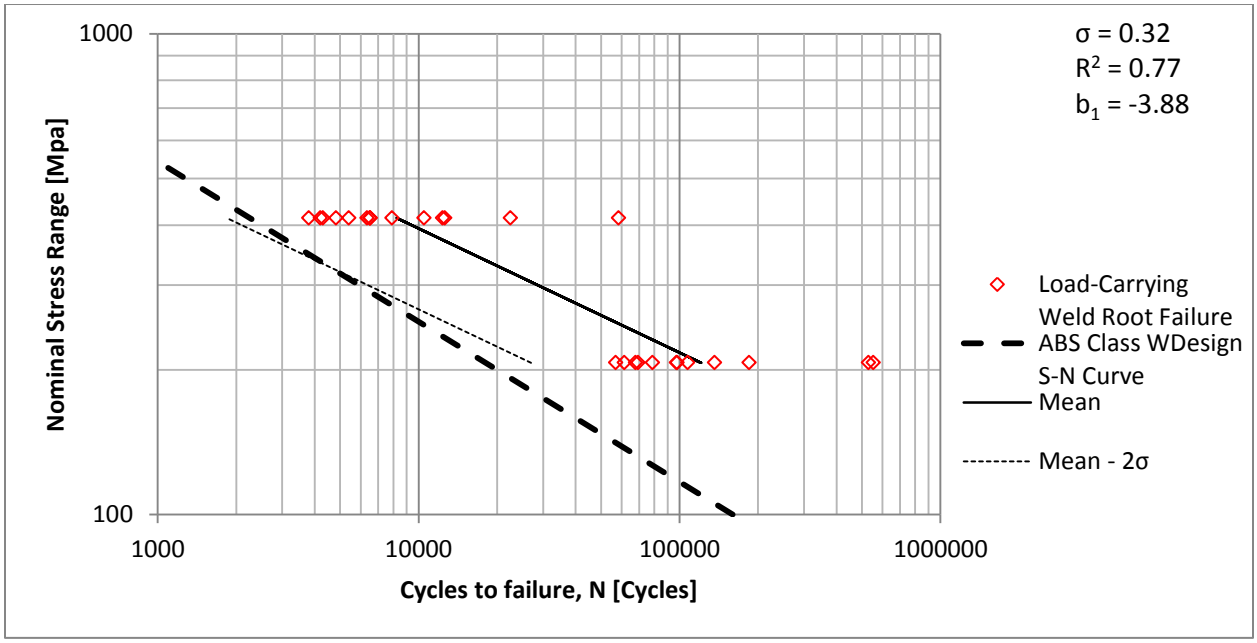

Figure 35: ABS Class W Design S-N Curve Vs. Experimental S-N Data of Load-Bearing Cruciform Joints with Weld Root Failure

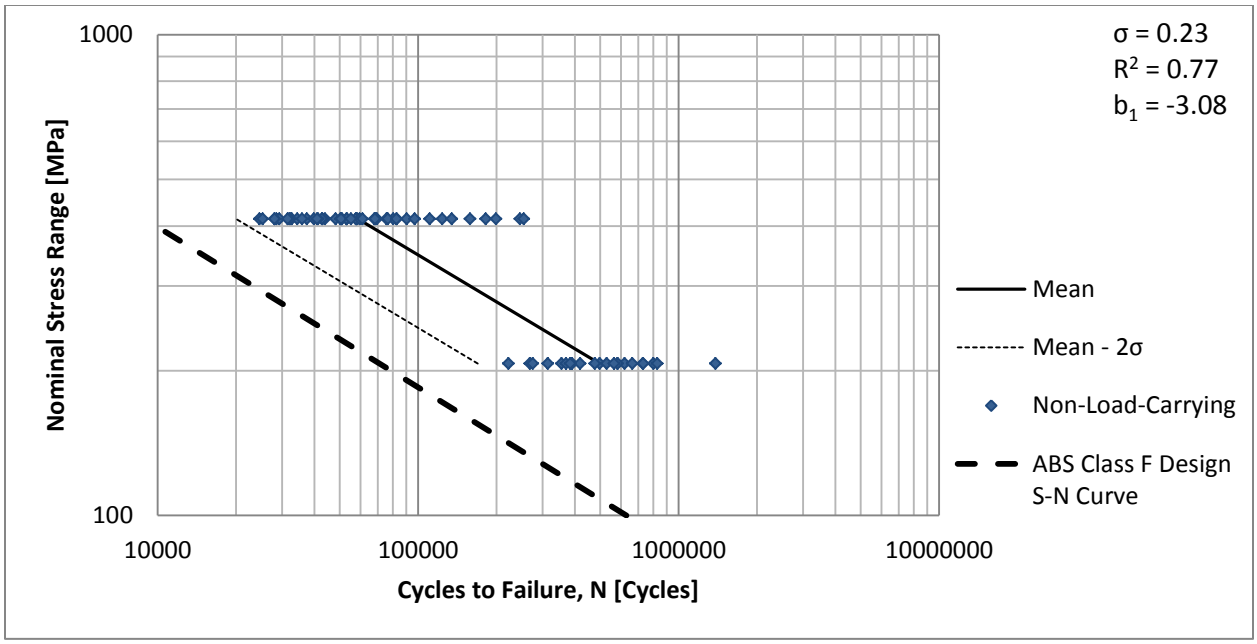

Figure 36: ABS Class F Design S-N Curve Vs. Experimental S-N Data of Non-Load-Bearing Cruciform Joints

Comparing the tested fatigue specimens, all the weld root and weld toe failures of load and non-load-carrying specimens exhibit higher fatigue lives than their respective corresponding ABS design curves . However, Class F design curve for non-load-carrying cruciform joints in Figure 36 seems over-conservative. The lower bound or the mean minus standard deviation curve of the actual test data falls higher than the design S-N curve. Nevertheless, the slope of the design curve, which is assumed equal to 3, is consistent with that of the experimental data.

Observing Class F2 and Class W design S-N curves in Figure 34 and Figure 35 respectively, the data lie well above the curves themselves validating the effectiveness of the ABS fatigue standards. Although the data more or less support the slopes of the ABS Class F2 and Class W design S-N curves, the slopes of the experimental data S-N curves tend to be steeper and overly conservative in the long life regime.

As discussed in the previous section, the structures with the thicknesses even below the reference thickness of 22 mm i.e. 5 mm and 10 mm display variations in the fatigue lives. Thus, there is a need to account for the thickness effect of the plates even below the reference thickness.

ABS design S-N curves serves as a good safety check for the fatigue assessment of any structures. Nevertheless, the data remain widespread with high standard deviations and low coefficient of correlation value. Therefore, an alternative approach is necessary to express the fatigue test results in the region of the test detail.

Limitations of Hot-Spot Stress for simple connections

The hot-spot stresses are expressed in terms of stress concentration factors, to be applied to nominal stresses. For the structures with weld details, in which the fatigue failure initiates from the weld toe, the structural stresses at the weld toe are called the hot-spot stresses. Nevertheless, when the failure occurs at the weld root, the hot-spot stress approach cannot be used. Thus, the application of hot-spot stress method is limited to the joint types with weld toe failure only. The hot-spot stresses include the stress concentration

effect due to the weld joint, but not due to the weld itself. Fatigue strength of several welded joints is hence represented by fewer curves.

For simple joints such as the cruciform joints, simple T-joints in plated structures or simple butt joints that are welded from one side only, the derivation of hot spot stress using finite element model with shell elements is not recommended. As shown in the figure below, the stresses in the direction I, or direction normal to the base plate shell, there is no stress flow into the transverse shell plating as it is represented by only one plane in the shell model. The analysis of such joints with shell model would give nominal stress even at the hot-spot locations. Thus, the hot-spot stress approach was not used to determine stress for the fatigue test specimens.

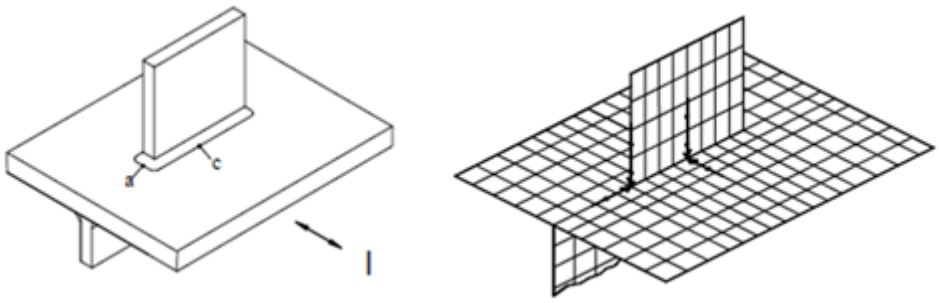

Figure 37: Illustration of Stress Normal to a Shell Element Model

According to the ABS fatigue design standard, when the stresses are obtained based on the hot-spot stress approach, the use of the ABS Offshore S-N Curve-Joint Class 'E' curve is recommended, for all the joint types. Class F, F2, and W S-N Curves characterize the load-carrying and non-load-carrying steel cruciform joints; the nominal stress S-N curve Class E, being higher than all three S-N curves, would be non-conservative to be used with the hot-spot stress approach.

IV. Master S-N Curve Representation

The conventional stress analysis method for the fatigue assessment of the welded joints is based on nominal stress or hot spot stress method. As witnessed earlier, the nominal stress based S-N plots exhibit poor data correlation and the widespread scatter of the data, and the hot-spot method based plots have shortcomings like mesh size sensitivity, arbitrariness of reference locations and failure to predict the fatigue behavior at times of weld root failures. Therefore, a new approach to the S-N curve representation is essential.

Nominal stress based S-N curves are basically parallel to one another, indicating the existence of a single S-N curve with all data collapsed into one single S-N curve, preferably straight. To establish such an S-N curve, a single effective global stress parameter is required, and the Master S-N Curve Approach introduced by Dr. Pingsha Dong and adopted by the new ASME Boiler & Pressure Vessel Code, Section VIII, Division 2, presents such scaling parameter in terms of equivalent structural stress.

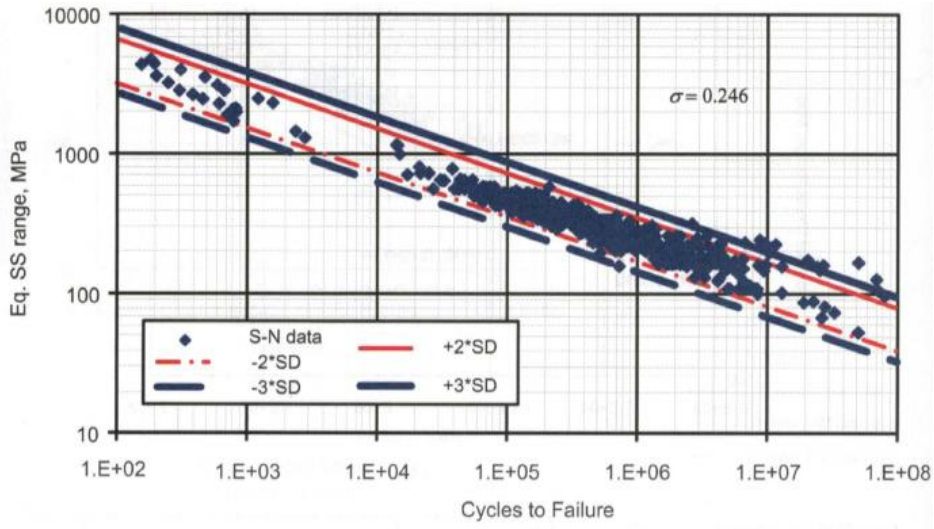

	Statistical Basis	C	h
$\Delta S_s = C \times N^h$	Mean	19930.2	-0.32
	$+2\sigma$	28626.5	
	-2σ	13578.8	
	$+3\sigma$	31796.1	
	-3σ	12492.6	

Figure 38: Master S-N Curve of Weldments and Statistical Representation of the Mean, Lower Bound, and Upper Bound Lines from WRC Bulletin

The Master S-N Curve is presented as by the equation below.

$$\Delta S_S = C.N^h \tag{8}$$

The constants C and h are derived from the regression analysis of large number of data shown in Figure 38.

Equivalent Structural Stress Parameter

The equivalent structural stress parameter is an effective global stress parameter, which is used as a basis to establish Master S-N Curve. It is represented by the following equation:

$$\Delta S_S = \frac{\Delta\sigma_S}{t^{*\frac{2-m}{2m}} I(r)^{\frac{1}{m}}} \quad (9)$$

The equivalent structural stress parameter (ΔS_S) is obtained by normalizing the structural stress range ($\Delta\sigma_S$), with two variable parameters, thickness (t) and the bending ratio (r) with m = 3.6, which is the value based on fracture mechanics concept. As a result, it explicitly captures three major aspects of the fatigue behavior in the welded joints that have been the topic of investigation.

i. Structural stress range ($\Delta\sigma_S$) captures the stress concentration effects of different joint types.
ii. The thickness correction term $t^{*\frac{2-m}{2m}}$ provides the scale or effective plate thickness (t) effects.
iii. The bending ratio term, or the loading mode function $I(r)^{\frac{1}{m}}$ captures the loading mode effects.

For the fatigue evaluations of welded joints, it is essential to observe the stress distribution at the fatigue prone locations rather than a stress value at a single point. When the crack travels or propagates, the stress alternates accordingly, hence the necessity of observing the stress distribution. The stress distribution at the fatigue failure location, such as weld toe is represented by two stress states simultaneously: an equilibrium-equivalent stress state and self-equilibrium stress state, as shown in figure below.

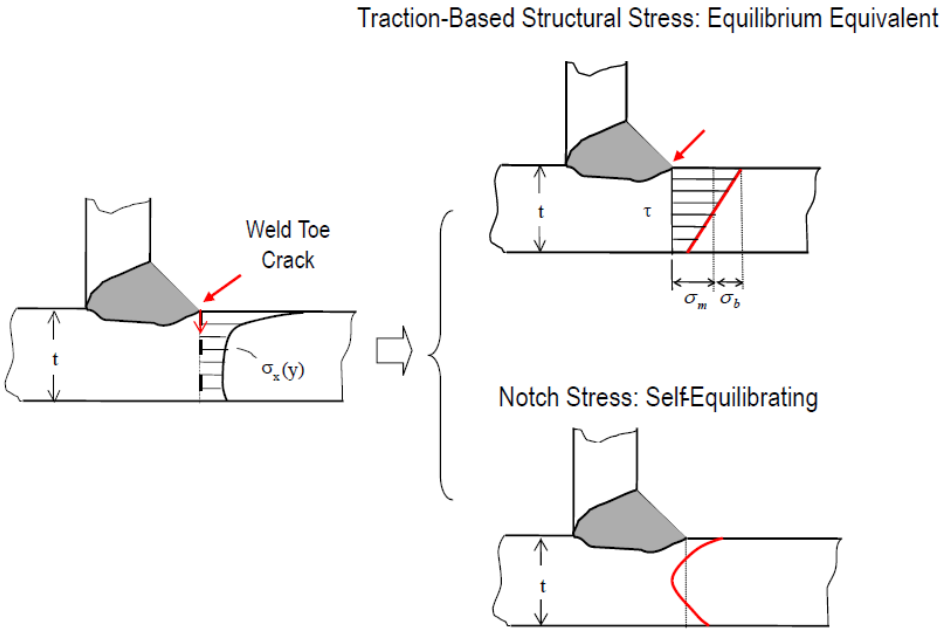

Figure 39: Through-thickness Structural Stresses Definition: Local Stresses, Structural Stress, and Self-Equilibrating Stress

Based on the fracture mechanics concept, the equilibrium-equivalent stress state or the traction-based stress state signifies a stress state that is similar to the corresponding equivalent far field stress state. While the self-

equilibrating stress state represents the stress state influenced by the local notch geometry. This stress is only dominant within a distance of 0.1t from the notch root. The thickness term and the bending ratio term then consider the self-equilibrating notch stress effect aspect in the Master S-N Curve.

Traction-Based Structural Stress

The traction-based structural stress definition is based on the elementary structural mechanics theory. It is a generalized nominal stress state at the fatigue prone location. Following considerations are made for the fatigue evaluations of the welded joints:

a. Since the local effects due to the weld geometry is already captured in S-N data, a global based stress measure is needed to exhibit the overall joint geometry effect along with the loading mode effect on overall stress concentration. Based on elementary structural mechanics principles, such parameter that captures the through-thickness distribution of stress state is in the form of membrane and bending stress. Membrane stress (σ_m) represents the uniform stress through the thickness whereas the bending stress (σ_b) represents the linear stress gradient in the stress state, as can be seen in Figure 39.

b. Three structural stress components are relevant to fatigue crack, corresponding to the linear representations of three traction components, along a hypothetical crack plane such as weld toe cracking. They are normal, in-plane shear, and transverse shear stresses, and the membrane and bending representation of these components satisfy the equilibrium conditions across and along the crack plane. See Figure 40.

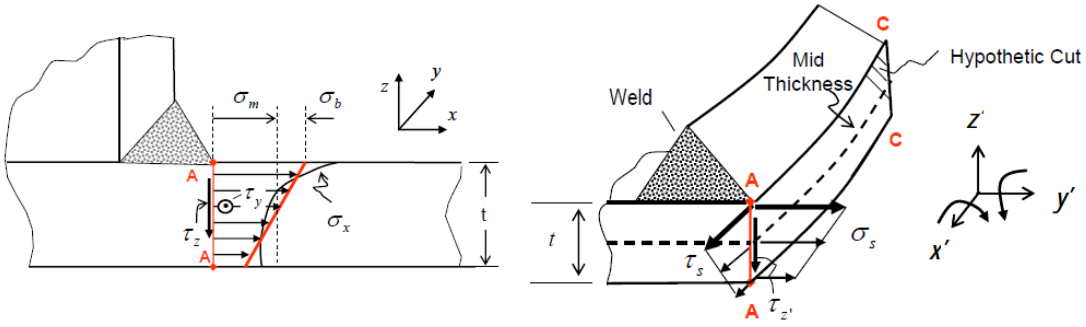

Figure 40: Exposing Three Structural Stress Components in Section A-A in a 2D Cross-Section (Left) and Section A-A-C-C in a 3D Cross-Section (Right)

c. The membrane and bending stresses are related to the line forces and the line moments. In FE analysis, the line forces and moments relate to nodal forces and moments according to the nodal force and displacement relationship. Displacement satisfies continuity in FE methods, thus the nodal forces as well. In the displacement based FE procedures, the nodal forces and displacements are considered to be the most fundamental quantities. The equilibrium conditions can be confirmed at the nodes only in terms of nodal forces, not in terms of stresses.

Therefore, the traction-based structural stress is based on the reaction forces at the nodes. It is determined using the nodal forces and moments along the hypothetical crack at the possible fatigue crack location, satisfying the equilibrium conditions.

Simplified Stress Formulation for 2D Analysis

Traction-based structural stress is by definition the summation of the membrane and the bending stress. Nodal forces are exposed with respect to the perpendicular direction to the weld line. Thus, with a view to maintain the equilibrium conditions, after extraction of nodal forces from the 2D FE model, the line force and the line moment per unit length through thickness are determined by utilizing following simplified equations.

$$f_x = \sum_{i=1}^{n} F_{xi} \quad (10)$$

$$m_z = \sum_{i=1}^{n} F_{xi} y_i \quad (11)$$

where, F_{xi} are the nodal forces from FE analysis at Nodes i
Y_i is the vertical distance of each node through thickness to a reference node
f_x and m_z are the line force and line moment.

For 2D models, the in-plane shear structural stress component is zero. Furthermore, the transverse shear stress is usually insignificant or its effect on fatigue behavior is negligible, hence it is ignored during calculation.

After determining the line forces and moments, the membrane and bending stresses are given by the following equations.

$$\sigma_m = \frac{f_x}{t} \quad (12)$$

$$\sigma_b = \frac{6m_z}{t^2} \quad (13)$$

where, σ_m is the membrane stress
σ_b is the bending stress
t is the plate thickness

Therefore, according to the structural mechanics theory, the traction-based structural stress(σ_S) is then characterized by,

$$\sigma_S = \sigma_m + \sigma_b \quad (14)$$

Also, the stress concentration factor (SCF_{SS}) based on traction-based structural stress is defined as the ratio of structural stress to the applied nominal stress (σ_n).

$$SCF_{SS} = \frac{\sigma_S}{\sigma_n} \quad (15)$$

In Case of Weld Root Failure

The traction based structural stress calculation for the weld throat (weld root failure) is similar as for the weld toe. Coordinate transformation is however required after collecting the nodal forces from the nodes along the weld throat line, as shown in Figure 41.

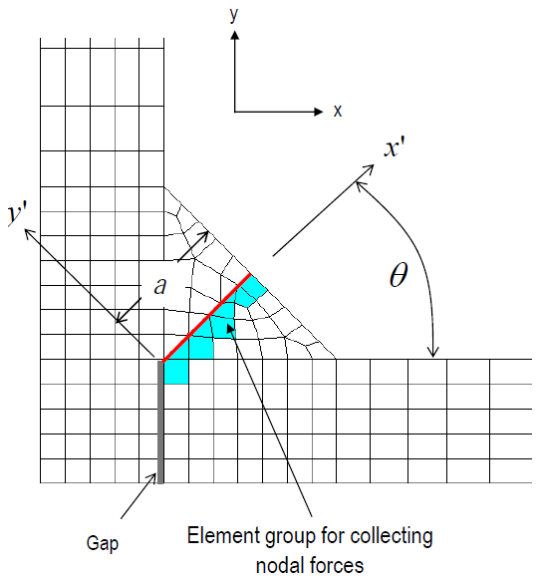

Figure 41: Element Group Highlighted to Collect the Nodal Forces for Weld Toe Failure

The collected nodal forces with respect to the global coordinate system (x,y) are rotated with respect to the angle θ into the local coordinate system (x', y'). Then the calculation is performed as usual.

$$F_{x'} = F_x Cos\theta + F_y Cos(90^\circ - \theta) \quad (16)$$

$$F_{y'} = -F_x Cos(90^\circ - \theta) + F_y Cos\theta \quad (17)$$

Then,

$$\sigma_S = \sigma_m + \sigma_b = \frac{1}{a}\sum_{i=1}^{n} F_{x'i} + \frac{6}{a^2}\sum_{i=1}^{n} F_{x'i} y_i \quad (18)$$

where, a is the length of the weld throat.

Self-Equilibrating Stress or Notch Stress

The remaining terms that are in the equivalent structural stress parameter help to account for the self-equilibrating part of the structural stress, and they are the thickness correction term and the loading mode function.

Loading mode function, $I(r)^{1/m}$ and Thickness Correction term, $t^{*(2-m)/2m}$

According to the two stage crack growth model based on fracture mechanics,

$$N = \int_{a\to 0}^{a=a_f} \frac{da}{C(M_{kn})^n (\Delta K)^m} \quad (19)$$

where K is the notch stress intensity factor
M_{kn} is the ratio of K with local notch effects and K based on through thickness (without notch intensity effect)
N is the fatigue life in cycles
a is the crack length

n = 2 (empirical constant)
m = 3.6 based on Paris law of crack propagation
C is the integration constant.

The above equation can be re-written in the relative crack length form as given below:

$$N = \int_{a/t\to 0}^{a/t=1} \frac{td(\frac{a}{t})}{C(M_{kn})^n (\Delta K)^m} = \frac{1}{C} t^{1-\frac{m}{2}} (\Delta\sigma_S)^{-m} I(r) \quad (20)$$

Thus, rearranging,

$$\Delta\sigma_S = C^{-1/m} . t^{\frac{2-m}{2m}} . I(r)^{1/m} . N \quad (21)$$

The loading mode function, I(r) is a dimensionless function of the bending ratio r, which is defined as the ratio of bending stress and the total structural stress ($r = \sigma_b/\sigma_S$). For pure membrane, r = 0 and similarly for pure bending, r = 1. $I(r)^{1/m}$, based on elliptical crack solution adopted by ASME Div 2 and API 579-1/ASME FFS-1, is given by the following empirical equation,

$$I(r)^{1/m} = 0.0011r^6 + 0.0767r^5 - 0.0988r^4 + 0.0946r^3 + 0.0221r^2 + 0.014r + 1.2223 \quad (22)$$

Similarly, the thickness correction term, $t^{*2-m/2m}$ indicates a penalty on stress range with increasing stress. t* however denotes a ratio of actual thickness t to a unit thickness, thus making the term dimensionless.

$$t^* = \frac{t}{t_{ref}} \quad (23)$$

where, t_{ref} = 1 mm in the Master S-N Curve. Note that the thickness 't' represents an effective thickness of the plate. For symmetric joint types, effective thickness is equal to half the thickness of the plate.

Fatigue Strength Assessment using Master S-N Curve Approach

After the nominal stress approach was utilized to correlate the fatigue data in S-N plots, the Master S-N curve approach was implemented to further inspect the effectiveness of this approach. In order to execute this approach, the traction-based structural stress was determined first for each specimen using finite element models in the finite element analysis software ABAQUS, and then, thickness correction as well as the loading mode function was later determined.

Finite Element Analysis and Structural Stress Calculation

As discussed earlier, the traction based structural stress is calculated by the following equation:

$$\sigma_S = \sigma_n \times SCF_{SS}$$

Based on the variations of nominal leg sizes and nominal thicknesses of each steel cruciform joints, there were sixteen (16) different finite element models, 8 load-carrying and 8 non-load-carrying specimens. The 5 mm thick cruciform had three different leg sizes, whereas, the 10 mm thick cruciform had five different leg sizes, as shown in the table below:

Table 9: Variation of the Cruciform Joints with respect to their Thicknesses and Weld Leg Sizes

Model(load & non-load)	Thickness, t [mm]	Weld Leg Size, s [mm]	s/t [-]
1	5	3	0.6
2	5	5	1.0
3	5	8	1.6
4	10	5	0.5
5	10	6	0.6
6	10	8	0.8
7	10	10	1.0
8	10	12	1.2

Due to the symmetry in the geometry, only a quarter of the cruciform joint was modeled, for the specimen with each thickness and corresponding weld leg size provided in the table. Four node, quadrilateral, plane strain elements, (denoted by CPE4 in ABAQUS) with mesh size as 0.5t x 0.5t was adopted to model the cruciform joints. Regarding the material property, the young's modulus of the model was set to be 207,900 MPa or 30,153 Ksi, and Poison ratio was 0.3. As an example of the procedure, a non-load-carrying cruciform joint of thickness = 10 mm, and weld size = 5 mm is presented below.

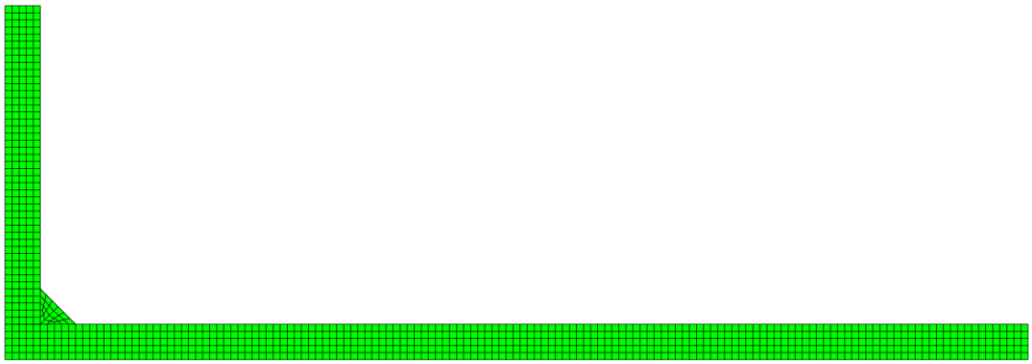

Figure 42: A Quarter FE Model of 10 mm Non-Load-Carrying Cruciform Joint

The boundary conditions were applied along the baseplate and the attachment plate symmetry line and uniform pressure load was applied to the end of the base plate as illustrated in Figure 43.

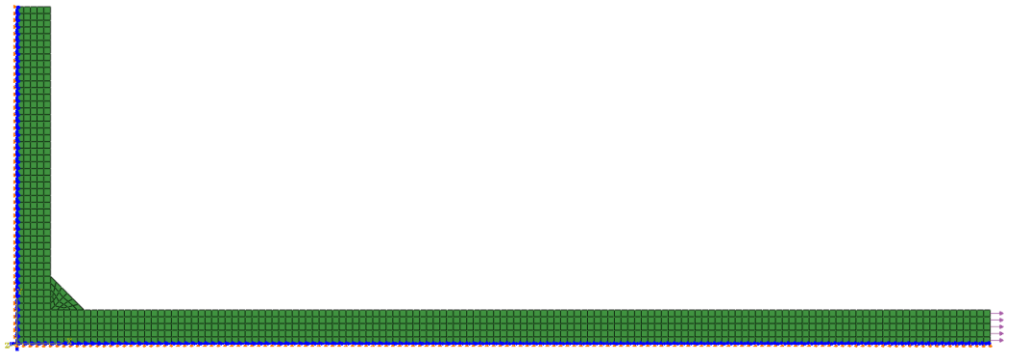

Figure 43: Boundary Conditions applied to the FE Model Along the Symmetry Lines

Along the horizontal symmetry line of the base plate, y-symmetry was implemented which means the model was restrained to move along y-axis, and rotate about z-axis. Similarly, along the vertical symmetry of the

attachment plate, x-symmetry was implemented which restrained the model to move along the x-axis, and again the rotation about z-axis.

Thus, finite element analysis was performed on the model above, and several other models with varying thicknesses and leg sizes.

The traction-based structural stress was calculated by making a hypothetical cut through the thickness of the base plate, at the weld toe for all the load-carrying and non-load-carrying specimens. However, for the load-carrying specimens, another hypothetical cut was made along the weld throat because of the possibility of the weld root failure in such joints. And nodal forces from the hypothetical cut location at the weld toe were then extracted.

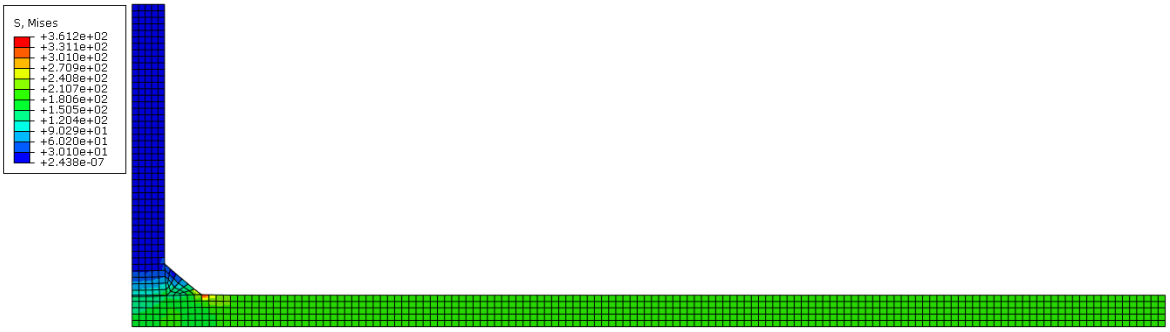

Figure 44: Von Mises Stress Distribution. Load Applied = 207 MPa.

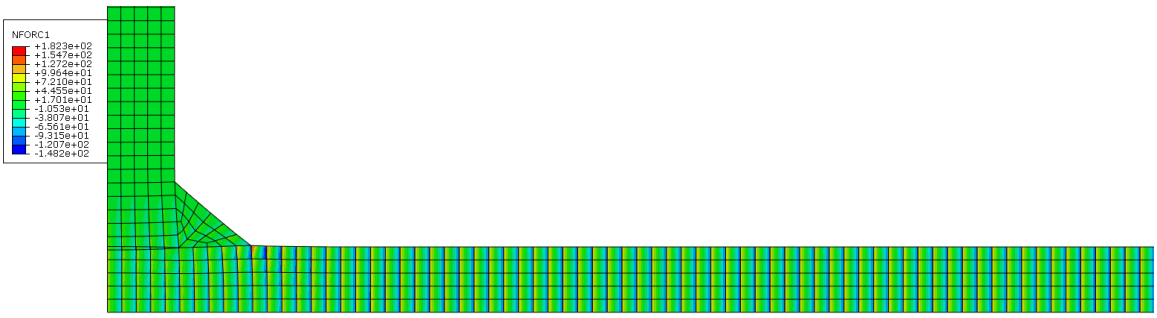

Figure 45: Nodal Force Distribution

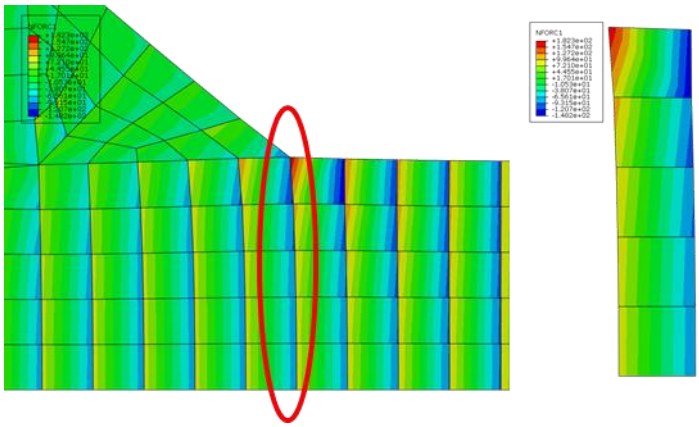

Figure 46: Hypothetical Cut Location at the Weld Toe through Thickness

Thus, collecting the elements at the right hand side of the hypothetical cut, following table specifies the elements and the node numbers, along with other parameters required to compute the traction based structural stress.

Table 10: Traction based Structural Stress Computation from FE Model

Element ID	Node ID	y_i	F_{xi} [N]	M_z [N/mm]	$f_x = \sum_{i=1}^{n} F_{xi} =$	1035 N
266	331	5	182.2630	455.6575	$m_z = \sum_{i=1}^{n} F_{xi}(y_i - \frac{t}{2}) =$	295.99 N/mm
	332	4	98.7151	148.0727		
267	332	4	118.0640	177.0960	$\sigma_m =$	206.999 MPa
	333	3	85.0535	42.5268	$\sigma_b =$	71.0379 MPa
268	333	3	103.4060	51.7030	$\sigma_s = \sigma_m + \sigma_b =$	278.04 MPa
	334	2	85.3294	-42.6647	Given, $\sigma_n =$	207 MPa
269	334	2	95.5064	-47.7532	$SCF_{SS} = \sigma_s/\sigma_n$	1.34
	335	1	86.6511	-129.9770	Effective thickness, t = 5 mm	
270	335	1	91.3552	-137.0330		
	336	0	88.656	-221.6400		

Stress Concentration Factor based on Traction Stress

Along with the traction stress based structural stresses, the stress concentration factors were simultaneously computed for the FE models. For a joint type, when the nominal stresses and SCF are known, then the structural stresses can be easily calculated. The SCF for models at fatigue prone locations, weld toe for load-carrying joints, and both weld toe and weld root for non-load-carrying joints were analyzed, and the parametric SCF curves were plotted as a function of s/t ratio. The curves in Figure 47 illustrate the relationship between SCF and s/t ratio, which was determined using ABAQUS.

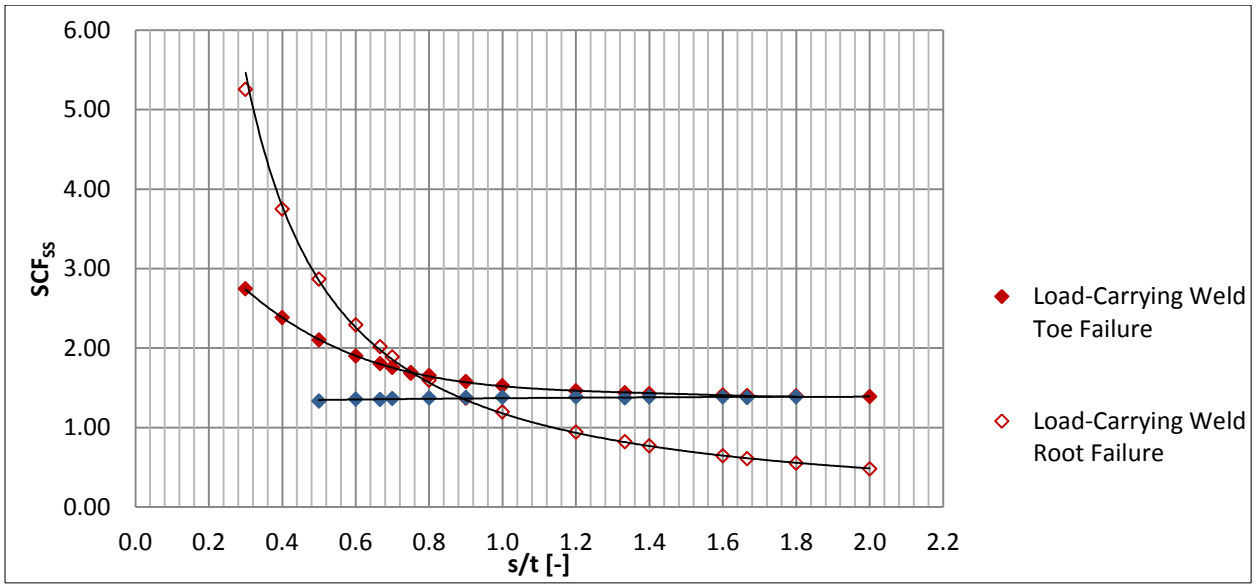

Figure 47: Parametric SCF Curves of Load-Carrying and Non-Load-Carrying Cruciform Joints

The figure demonstrates for load-carrying joints, SCF decreases as s/t ratio increases, but, for the non-load-carrying joints, it is the opposite. However, compared to the load-carrying joints' curves, there is no remarkable fluctuation in the SCF values of non-load-carrying joints as s/t ratio varies. Furthermore, observing the two curves for load-carrying specimens, the figure confirms an intersection point of the two curves at an approximate value of s/t ratio equal to 0.75. It is obvious that higher the SCF, greater the possibility of fatigue crack. Thus, Figure 47 indicates that for the specimens with s/t approximately smaller than 0.75, weld root failure dominates the fatigue behavior, and those with SCF higher than 0.75, the weld toe failure mode will be dominant. These curves establish the validity of experimental data in Figure 27 and Figure 28.

Equivalent Structural Stress Based Experimental S-N Chart

If all the fatigue test data of the load-carrying as well as non-load-carrying cruciforms, with weld root along with the weld toe failure can be put together into one single narrow band on the S-N chart, then this would ultimately prove the validity of the Master S-N Curve and hence, the equivalent structural stress parameter. As already discussed in the sections above, the equivalent structural stress, which is the basis of Master S-N curve is given by,

$$\Delta S_S = \frac{\Delta\sigma_n SCF_{ss}}{t^{*\frac{2-m}{2m}} I(r)^{\frac{1}{m}}}$$

where $\Delta\sigma_n$ is the applied nominal stress range
SCF_{ss} is the traction based structural stress concentration factor
$t^{(2-m)/2m}$ is the thickness correction term
$I(r)^{1/m}$ is the loading mode function with m = 3.6

The bending ratio r is given by: $r = \Delta s_b / \Delta s_S$

The loading mode function $I(r)^{1/m}$ is given by:
$I(r)^{1/m} = 0.0011r^6 + 0.0767r^5 - 0.0988r^4 + 0.0946r^3 + 0.0221r^2 + 0.014r + 1.2223$

Thus, after the calculation of traction based structural stress for each set of the specimens with FE models, the thickness correction values and loading mode functions were determined. The calculated bending stresses for all the specimens were more or less constant, and the approximate value of loading mode function $I(r)^{1/m}$ for all the specimens was 1.23. Thus, for the test specimens,

$I(r)^{1/m} = 1.23$

The thickness correction value for 5 mm and 10 mm thick base plate specimens were determined to be 0.707 and 0.606 respectively.

Hence, using the estimated values for all the load-carrying and non-load-carrying fatigue test specimens, the equivalent structural stress parameter for each individual tested specimen was computed, and thus, plotted against the cycles to failure as below:

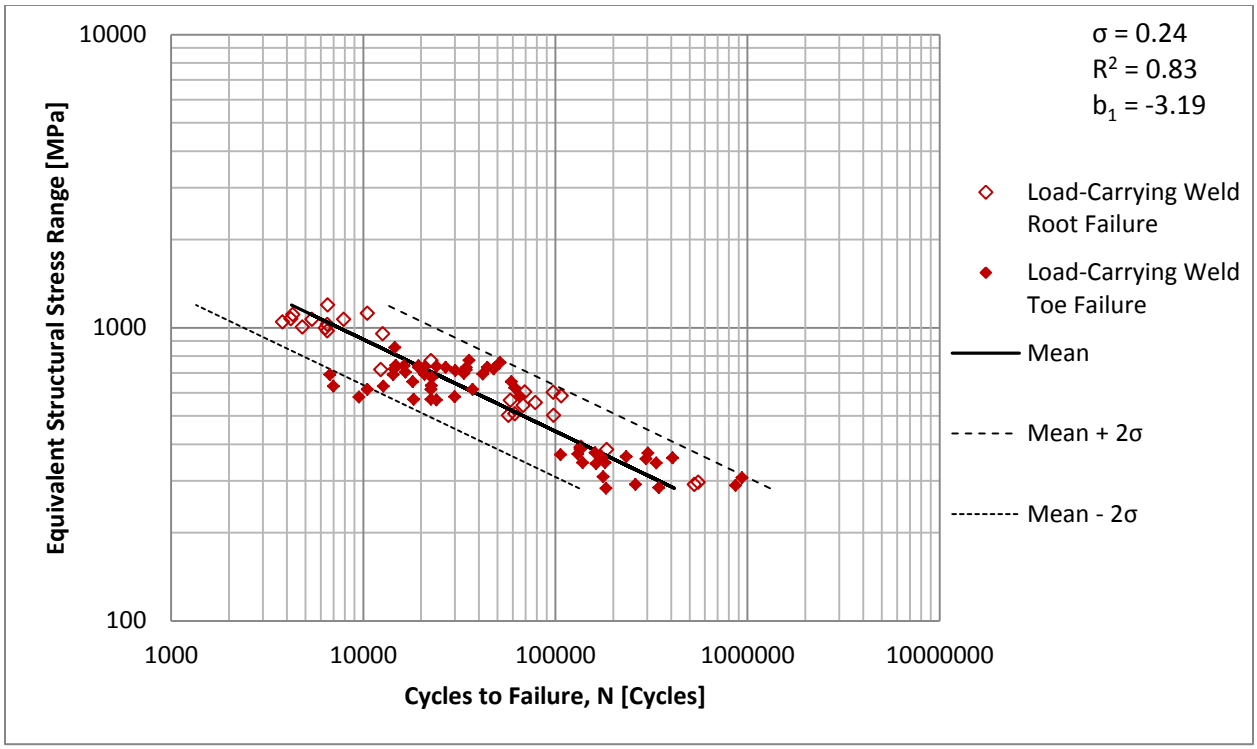

Figure 48: Equivalent Structural Stress based S-N Chart for Load-Carrying Specimens

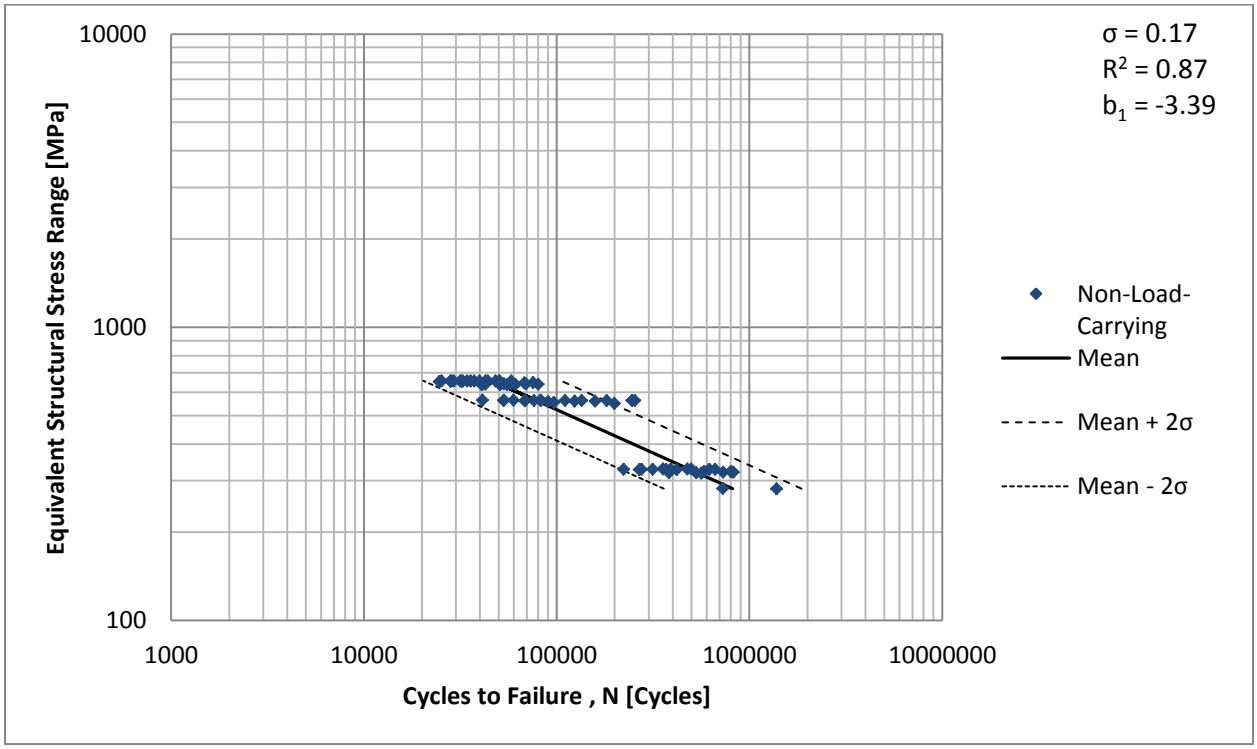

Figure 49: Equivalent Structural Stress based S-N Chart for Non-Load-Carrying Specimens

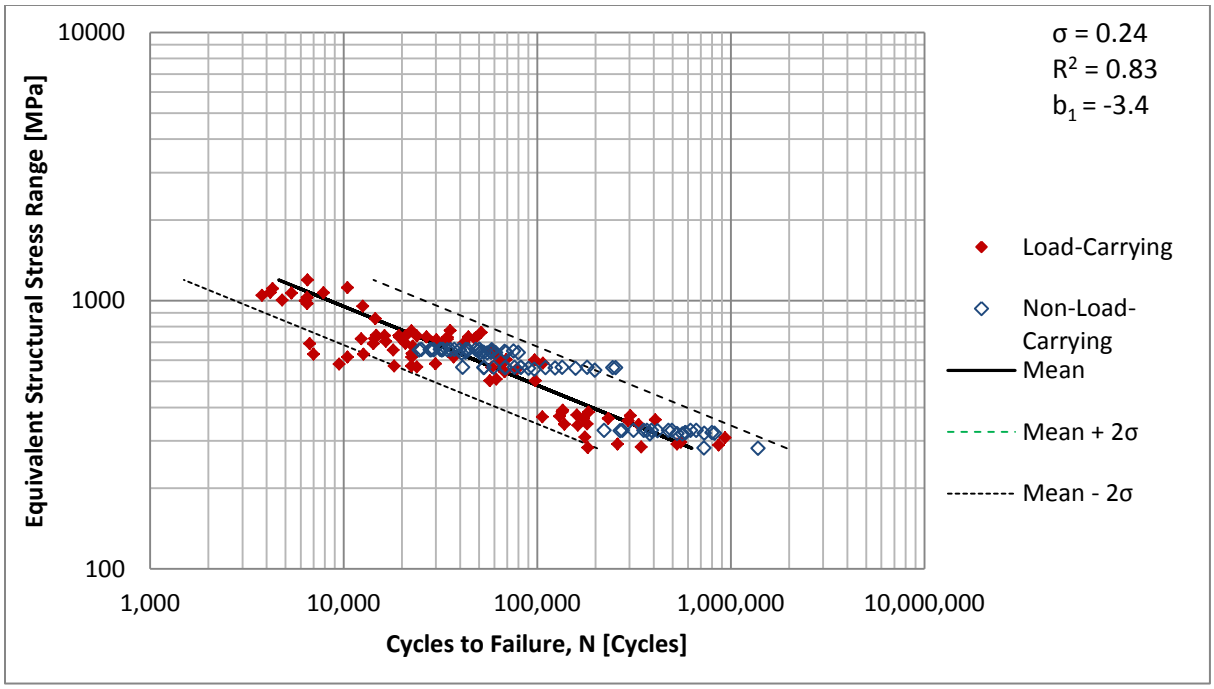

Figure 50: Equivalent Structural Stress based S-N Chart for Load-Carrying and Non-Load-Carrying Specimens

Statistical Parameter Comparison of S-N plots based on Equivalent Structural Stress with Nominal Stress Approach

As demonstrated by Figure 48, Figure 49, and Figure 50, all the S-N data, based on the equivalent structural stresses calculated using FE models, reasonably correlate and collapse into a narrower band, irrespective of the cruciform joint types, plate thicknesses, and weld sizes when compared to the nominal stress based S-N Plots. For clarification purpose, following tables include the values of main statistical parameters helpful to investigate the correlation of the data points in the fatigue assessment based on both nominal stress and equivalent structural stress parameter.

Table 11: Comparison of Statistical Parameters of S-N Curves based on Nominal Stress and Equivalent Structural Stress

Load-Carrying Steel Cruciform Joints

Stress Approach	**σ**	**r^2**	**b_1**
Nominal	0.33	0.70	-3.40
Equivalent Structural	0.24	0.83	-3.19

Load-Carrying & Non-Load-Carrying Cruciform Joints

Stress Approach	**σ**	**r^2**	**b_1**
Nominal	0.38	0.58	-3.12
Equivalent Structural	0.24	0.83	-3.40

Non-Load-Carrying Steel Cruciform Joints

Stress Approach	**σ**	**r^2**	**b_1**
Nominal	0.23	0.77	-3.08
Equivalent Structural	0.17	0.87	-3.39

In Table 11, the standard deviation values of load-carrying, non-load-carrying, and both load and non-load carrying joints specimen data together, were 0.33, 0.23, and 0.38 respectively when the nominal stresses were plotted in the S-N chart. However, significant reduction of the values followed when instead of equivalent structural stresses replaced the nominal stresses. The standard deviation values dropped from 0.33 to 0.24 for load-carrying joints data, 0.23 to 0.17 for non-load-carrying joints data, and 0.38 to 0.24 for both load and non-load-carrying joints data put together. The substantial reduction in standard deviation indicates the strong correlation of the data points and possibility of a single master S-N curve. Similarly, the r-squared values increased with the use of equivalent structural stress parameter over the nominal stress. The closer the value of R^2 to 1, the better the regression line fits the data set. From the numerical values of R^2 in the provided table, the equivalent structural approach has higher values, ranging from 0.83 to 0.87, and hence, gives better curve fit.

Comparing all the standard deviation and R^2 values in the table above, it can be concluded that there existed the least correlation when the load-carrying and non-load-carrying specimens fatigue data were put together in an S-N plot based on nominal stress approach. However, with the use of equivalent structural stress, the standard deviation is reasonably lowered and the correlation is remarkably improved.

Conclusion

Not only can the traction based structural stress parameter be calculated consistently with the provided traction stress approach, but it also serves an effective fatigue parameter in order to correlate the fatigue behavior of welded joints irrespective of the joint types, plate thicknesses, the weld sizes along with the loading modes. When associated with the fracture mechanics concept, a master S-N curve can be generated with the basis of equivalent structural stress parameter. This parameter captures the geometric stress concentration factor, the loading mode, and the plate thickness effects in different kind of joints, and consequently, provides a significant improvement in the correlation of fatigue data. Thus, the master S-N curve approach, along with the application of equivalent structural stress concept, serves as a good platform for effective fatigue assessment of welded joints in the ships and offshore structures.

V. Conclusions

In this study, a brief literature review of the ABS Publication 115, Guide for The Fatigue Assessment of Offshore Structures, was performed. Further, the fatigue tests were performed on the load-carrying and non-load-carrying cruciform weld details, typical in marine structures. The experimental results were subsequently evaluated, and compared with the ABS fatigue assessment methods. Finally, the master S-N Curve approach was utilized, and the experimental data were evaluated using the equivalent structural stress parameter. The findings of this study can be summarized as follows.

i. Nominal stress definition is consistent; however, the determination of nominal stresses in the complex structures is a challenge in itself. There is virtually no correlation in the S-N data based on nominal stress approach.

ii. Hot-Spot stress approach reduces the number of eight S-N curves to a single class "E" S-N curve. However, hot-spot stress, when determined using FE model, is sensitive to the element type and the mesh size, thus, it is not consistent. In addition, in its calculation procedure, no clear justification to the reference locations, 0.5t and 1.5t, is provided. This approach is not applicable to the FE models of simple connections like cruciform joints.

iii. Experimental results indicate that the fatigue lives of the structures vary with the variation in the thicknesses of the base plates, even if the thickness is lower than the reference thickness provided in ABS guidelines.

iv. The load-carrying steel cruciform joints have two fatigue failure modes: weld root failure and weld toe failure, whereas, the non-load-carrying steel cruciform joints have only weld toe failures. The stress concentration curves developed from the finite element models of the cruciform joints display a critical point for the load-carrying joints where the failure mode transitions from weld root to weld toe, and that point is in the vicinity of s/t ratio = 0.75.

v. The equivalent structural stress is consistent with the master S-N curve, and it correlates the fatigue experimental data reasonably well. It takes into account the influence of thickness as well as loading mode variations, and considers the stress concentration factor of different geometry. Thus, this parameter makes it possible to plot the fatigue data of several joint types of varying thicknesses and loading modes into a single S-N chart, with relatively narrow scatter band. Overall, in fatigue evaluation methods, the equivalent structural stress serves as a very good fatigue parameter.

References

"Commentary on the Guide for the Fatigue Assessment of Offshore Structures," ABS, April, 2003.

"Fatigue Design of Offshore Steel Structures," DNV RP-C203, April 2010.

"Guide for the Fatigue Assessment of Offshore Structures," ABS, April, 2003.

Doerk, O., Fricke, W., and Weissenborn, C., "Comparison of Different Calculation Methods for Structural Stresses at Welded Joints," International Journal of Fatigue, Vol. 25, pp.359-369, 2003.

Dong, P., Hong, J.K., Osage, D.A., Dewees, D.J., and Prager, M., "Master S-N Curve Method An Implementation for Fatigue Evaluation of Welded Components in the ASME B&PV Code, Section VIII, Division 2, and API 579-1/ASME FFS-1, Welding Research Council Bulletin, No. 523, 2010, New York, New York.

Dong, P., "Verity Weld Fatigue Method in Fe-Safe Using ANSYS," Columbus, Ohio.

Fricke, W., and Kahl, A., "Comparison of Different Structural Stress Approaches for Fatigue Assessment of Welded Ship Structures," Marine Structures, Vol. 18, pp.473-488, 2005.

Fricke, W., "Fatigue Analysis of Welded Joints: State of Development," Marine Structures, Vol. 16, pp.185-200, 2003.

Huang, T.D., Harbison, M., Kvidahl, L., Niolet, D., Walks, J., Stefanick, K., Phillipi, M., Dong, p., DeCan, L., Caccese, V., Blomquist, P., Kihl, D., Wong, R., Nappi, N., gardner, J., Wong, C., Bjornson, M., and Manuel, A., "Overwelding and Distortion Control for Naval Surface Combatants," SNAME Journal of……..

Iwata, T and Matsuoka, K., "Fatigue Strength of CP Grade 2 Titanium Fillet Welded Joint for Ship Structure," Welding in the world, Vol. 48, No.7-8, pp.40-47, 2004.

Kihl, D.P. and Sarkani, S., "Thickness Effects on the Fatigue Strength of Welded Steel Cruciforms," International Journal of Fatigue, Vol. 19, No. 1, pp. S311-S316, 199, Great Britain.

Kim, M.H., Kang, S.W., Kim, J.H. Kim, K.S., Kang, J.K., and Heo, J.H., "An Experimental Study on the Fatigue Strength Assessment of Longi-Web Connections in Ship Structures Using Structural Stress," International Journal of Fatigue, Vol. 32, pp.318-329, 2010.

Maddox, S.J., "Recommended Hot-Spot Stress Design S-N Curves for Fatigue Assessment of FPSOs," Proceedings of International Journal of Offshore and Polar Engineering, June 17-22, 2001, Stavanger, Norway.

Maddox, S.J., "Fatigue Design Rules for Welded Structures," Progress in Structural Engineering and Materials, Vol. 2, No. 1, pp. 102-109, Jan-Mar, 2000.

Maddox, S.J., "Review of Fatigue Assessment Procedures for Welded Aluminum Structures," International Journal of Fatigue, Paper JIJF1005, Vol. 25, No. 12, pp. 1359-1378, December, 2003.

Schijve, J., "Fatigue of Structures and Materials in the 20th Century and the State of the Art," International Journal of Fatigue, Vol. 25, pp.679-702, 2003.

Wang, X. and Cheng, Z., "Sensitivity of Fatigue Assessment to the Use of Different Reference S-N Curves," Proceedings of 22nd International Conference on Offshore Mechanics and Arctic Engineering, June 8-13, 2003, Cancun, Mexico.

Appendices

Appendix A

ABS

APPENDIX 1 Guidance on Structural Detail Classifications for Use with ABS Offshore S-N Curves*

Type number, description and notes on mode of failure	*Class*	*Explanatory comments*	*Examples, including failure modes*
TYPE 1 MATERIAL FREE FROM WELDING			
Notes on potential modes of failure In plain steel, fatigue cracks initiate at the surface, usually either at surface irregularities or at corners of the cross-section. In welded construction, fatigue failure will rarely occur in a region of plain material since the fatigue strength of the welded joints will usually be much lower. In steel with rivet or bolt holes or other stress concentrations arising from the shape of the member, failure will usually initiate at the stress concentration.			
1.1 **Plain steel**			
(a) In the as-rolled condition, or with cleaned surfaces but with no flame-cut edges of re-entrant corners.	B	Beware of using Class B for a member which may acquire stress concentrations during its life, e.g. as a result of rust pitting. In such an event Class C would be more appropriate.	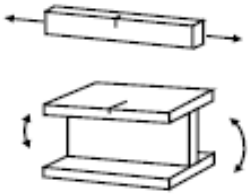
(b) As (a) but with any flame-cut edges subsequently ground or machined to remove all visible sign of the drag lines.	B	Any re-entrant corners in flame-cut edges should have a radius greater than the plate thickness.	
(c) As (a) but with the edges machine flame-cut by a controlled procedure to ensure that the cut surface is free from cracks.	C	Note, however, that the presence of a re-entrant corner implies the existence of a stress concentration so that the design stress should be taken as the net stress multiplied by the relevant stress concentration factor.	
TYPE 2 CONTINUOUS WELDS ESSENTIALLY PARALLEL TO THE DIRECTION OF APPLIED STRESS			
Notes on potential modes of failure With the excess weld metal dressed flush, fatigue cracks would be expected to initiate at weld defect locations. In the as-welded condition, cracks might initiate at stop-start positions or, if these are not present, at weld surface ripples. **General comments** *i)* **Backing strips** If backing strips are used in making these joints: (a) they must be continuous, and (b) if they are attached by welding those welds must also comply with the relevant Class requirements (note particularly that tack welds, unless subsequently ground out or covered by a continuous weld, would reduce the joint to Class F, see joint 6.5). *ii)* **Edge distance** An edge distance criterion exists to limit the possibility of local stress concentrations occurring at unwelded edges as a result, for example, of undercut, weld spatter, or accidental overweave in manual fillet welding (see also notes on joint Type 4). Although an edge distance can be specified only for the 'width' direction of an element, it is equally important to ensure that no accidental undercutting occurs on the unwelded corners of, for example, cover plates or box girder flanges. If it does occur it should subsequently be ground smooth.			
2.1 Full or partial penetration butt welds, or fillet welds. Parent or weld metal in members, without attachments, built up of plates or sections, and joined by continuous welds.			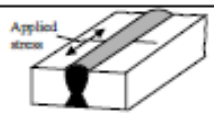

* The contents of Appendix 1 have been adapted from publications of the U.K. Health and Safety Executive. Permission from the Health and Safety Executive to use the source material is gratefully acknowledged.

Type number, description and notes on mode of failure	*Class*	*Explanatory comments*	*Examples, including failure modes*
(a) Full penetration butt welds with the weld overfill dressed flush with the surface and finish-machined in the direction of stress, and with the weld proved free from significant defects by nondestructive examination.	B	The significance of defects should be determined with the aid of specialist advice and/or by the use of fracture mechanics analysis. The NDT technique must be selected with a view to ensuring the detection of such significant defects.	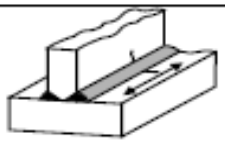
(b) Butt or fillet welds with the welds made by an automatic submerged or open arc process and with no stop-start positions within the length.	C	If an accidental stop-start occurs in a region where Class C is required remedial action should be taken so that the finished weld has a similar surface and root profile to that intended.	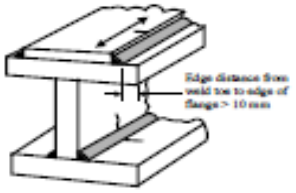
(c) As (b) but with the weld containing stop-start positions within the length.	D	For situation at the ends of flange cover plates see joint Type 6.4.	

TYPE 3 TRANSVERSE BUTT WELDS IN PLATES (i.e. essentially perpendicular to the direction of applied stress)

Notes on potential modes of failure

With the weld ends machined flush with the plate edges, fatigue cracks in the as-welded condition normally initiate at the weld toe, so that the fatigue strength depends largely upon the shape of the weld overfill. If this is dressed flush the stress concentration caused by it is removed and failure is then associated with weld defects. In welds made on a permanent backing strip, fatigue cracks initiate at the weld metal/strip junction, and in partial penetration welds (which should not be used under fatigue conditions), at the weld root
Welds made entirely from one side, without a permanent backing, require care to be taken in the making of the root bead in order to ensure a satisfactory profile.

Design stresses

In the design of butt welds of Types 3.1 or 3.2 which are not aligned the stresses must include the effect of any eccentricity. An approximate method of allowing for eccentricity in the thickness direction is to multiply the normal stress by $(1 + 3\ e/t)$, where e is the distance between centers of thickness of the two abutting members; if one of the members is tapered, the center of the untapered thickness must be used, and t is the thickness of the thinner member.

With connections which are supported laterally, e.g. flanges of a beam *which* are supported by the web, eccentricity may be neglected.

3.1 Parent metal adjacent to, or weld metal in, full penetration butt joints welded from both sides between plates of equal width and thickness or where differences in width and thickness are machined to a smooth transition not steeper than 1 in 4.		Note that this includes butt welds which do not completely traverse the member, such as welds used for inserting infilling plates into temporary holes.	
(a) With the weld overfill dressed flush with the surface and with the weld proved free from significant defects by non-destructive examination.	C	The significance of defects should be determine with the aid of specialist advice and/or by the use of fracture mechanics analysis. The NDT technique must be selected with a view to ensuring the detection of such significant defects.	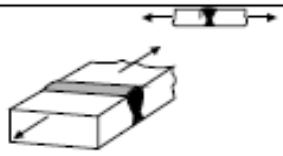
(b) With the welds made, either manually or by an automatic process other than submerged arc, provided all runs are made in the downhand position.	D	In general welds made by the submerged arc process, or in positions other than downhand, tend to have a poor reinforcement shape, from the point of view of fatigue strength. Hence such welds are downgraded from D to E.	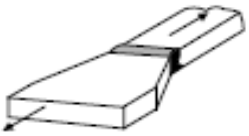
(c) Welds made other than in (a) or (b).	E	In both (b) and (c) of the corners of the cross-section of the stressed element at the weld toes should be dressed to a smooth profile. Note that step changes in thickness are in general, not permitted under fatigue conditions, but that where the thickness of the thicker member is not greater than 1.15 × the thickness of the thinner member, the change can be accommodated in the weld profile without any machining. Step changes in width lead to large reductions in strength (see joint Type 3.3).	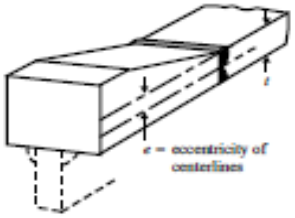

Type number, description and notes on mode of failure	*Class*	*Explanatory comments*	*Examples, including failure modes*
3.2 Parent metal adjacent to, or weld metal in, full penetration butt joints made on a permanent backing strip between plates of equal width and thickness or with differences in width and thickness machined to a smooth transition not steeper than 1 in 4.	F	Note that if the backing strip is fillet welded or tack welded to the member the joint could be reduced to Class G (joint Type 4.2).	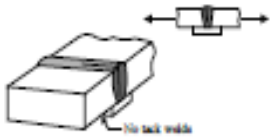
3.3 Parent metal adjacent to, or weld metal in, full penetration butt welded joints made from both sides between plates of unequal width, with the weld ends ground to a radius not less than 1.25 times the thickness t.	F2	Step changes in width can often be avoided by the use of shaped transition plates, arranged so as to enable butt welds to be made between plates of equal width. Note that for this detail the stress concentration has been taken into account in the joint classification.	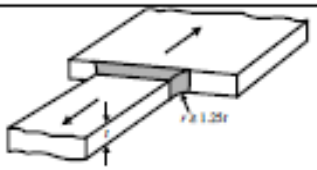
TYPE 4 WELDED ATTACHMENTS ON THE SURFACE OR EDGE OF A STRESSED MEMBER			
Notes on potential modes of failure			
When the weld is parallel to the direction of the applied stress fatigue cracks normally initiate at the weld ends, but when it is transverse to the direction of stressing they usually initiate at the weld toe; for attachments involving a single, as opposed to a double weld, cracks may also initiate at the weld root. The cracks then propagate into the stressed member. When the welds are on or adjacent to the edge, of the stressed member the stress concentration is increased and the fatigue strength is reduced; this is the reason for specifying an 'edge distance' in some of these joints (see also note on edge distance in joint Type 2).			
4.1 Parent metal (of the stressed member) adjacent to toes or ends of bevel-butt or fillet welded attachments, regardless of the orientation of the weld to the direction of applied stress, and whether or not the welds are continuous round the attachment.		Butt welded joints should be made with an additional reinforcing fillet so as to provide a similar toe profile to that which would exist in a fillet welded joint.	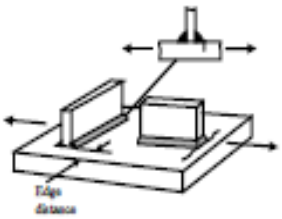
(a) With attachment length (parallel to the direction of the applied stress) ≤ 150 mm and with edge distance ≥ 10 mm.	F	The decrease in fatigue strength with increasing attachment length is because more load is transferred into the longer gusset giving an increase in stress concentration.	
(b) With attachment length (parallel to the direction of the applied mass) >150 mm and with edge distance. ≥ 10 mm.	F2		
4.2 Parent metal (of the stressed member) at the toes or the ends of butt or fillet welded attachments on or within 10 mm of the edges or corners of a stressed member, and regardless of the shape of the attachment.	G	Note that the classification applies to all sizes of attachment. It would therefore include, for example, the junction of two flanges at right angles. In such situations a low fatigue classification can often be avoided by the use of a transition plate (see also joint Type 3.3).	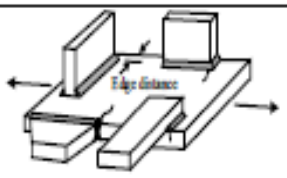
4.3 Parent metal (of the stressed member) at the toe of a butt weld connecting the stressed member to another member slotted through it.		Note that this classification does not apply to fillet welded joints (see joint Type 5.1b). However it does apply to loading in either direction (L or T in the sketch).	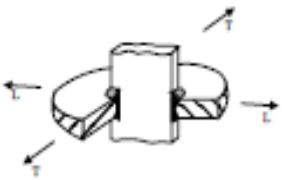
(a) With the length of the slotted-through member, parallel to the direction of the applied stress, ≤ 150 mm and edge distance ≥ 10 mm.	F		
(b) With the length of the slotted-through member, parallel to the direction of the applied stress, > 150 mm and edge distance ≥ 10 mm.	F2		
(c) With edge distance < 10 mm.	G		

Type number, description and notes on mode of failure	*Class*	*Explanatory comments*	*Examples, including failure modes*
TYPE 5 LOAD-CARRYING FILLET AND T BUTT WELDS			
Notes on potential modes of failure Failure in cruciform or T joints with full penetration welds will normally initiate at the weld toe, but in joints made with load-carrying fillet or partial penetration butt welds cracking may initiate either at the weld toe and propagate into the plate or at the weld root and propagate through the weld. In welds parallel to the direction of the applied stress, however, weld failure is uncommon; cracks normally initiate at the weld end and propagate into the plate perpendicular to the direction of applied stress. The stress concentration is increased, and the fatigue strength is therefore reduced, if the weld end is located on or adjacent to the edge of a stressed member rather than on its surface.			
5.1 **Joint description** Parent metal adjacent to cruciform joints or T joints (member marked X in sketches		Member Y can be regarded as one with a non-load-carrying weld (see joint Type 4.1). Note that in this instance the edge distance limitation applies.	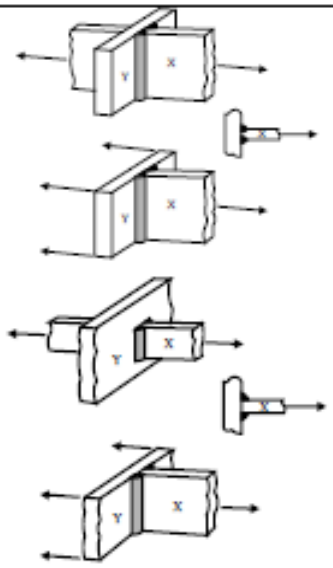
(a) Joint made with full penetration welds and with any undercutting at the corners of the member dressed out by local grinding.	F		
(b) Joint made with partial penetration or fillet welds with any undercutting at the corners of the member dressed out by local grinding.	F2	In this type of joint, failure is likely to occur in the weld throat unless the weld is made sufficiently large (see joint Type 5.4).	
5.2 Parent metal adjacent to the toe of load-carrying fillet welds which are essentially transverse to the direction of applied stress (member X in sketch).		The relevant stress in member X should be calculated on the assumption that its effective width is the same as the width of member Y.	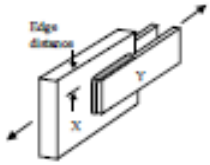
(a) Edge Distance ≥ 10 mm.	F2	These classifications also apply to joints with longitudinal welds only.	
(b) Edge Distance < 10 mm.	G		
5.3 Parent metal at the ends of load-carrying fillet welds which are essentially parallel to the direction of applied stress. with the weld end on plate edge (member Y in sketch).	G		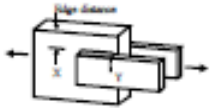
5.4 Weld metal in load-carrying joints made with fillet or partial penetration welds, with the welds either transverse or parallel to the direction of applied stress (based on nominal shear stress on the minimum weld throat area).	W	This includes joints in which a pulsating load may be carried in bearing, such as the connection of bearing stiffeners of flanges. In such examples the welds should be designed on the assumption that none of the load is carried in bearing.	
TYPE 6 DETAILS IN WELDED GIRDERS			
Notes on potential modes of failure Fatigue cracks generally initiate at weld toes and are especially associated with local stress concentrations at weld ends, short lengths of return welds, and changes of direction. Concentrations are enhanced when these features occur at or near an edge of a part (see notes on joint Type 4).			
General comment Most of the joints in this section are also shown, in a more general form, in joint Type 4; they are included here for convenience as being the joints which occur most frequently in welded girders. Where edge distance is mentioned in the joint types below, it refers to the distance from a free (unwelded) edge.			

Type number, description and notes on mode of failure	*Class*	*Explanatory comments*	*Examples, including failure modes*
6.1 Parent metal at the toe of a weld connecting a stiffener, diaphragm, etc. to a girder flange.		Edge distance refers to distance from a free, i.e. unwelded, edge. In this example, therefore, it is not relevant as far as the (welded) edge of the	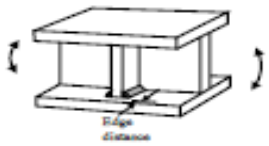
(a) Edge distance ≥ 10mm (see joint Type 4.2).	F	Web plate is concerned. For reason for edge distance see note on joint	
(b) Edge Distance < 10 mm.	G	Type 2.	
6.2 Parent metal at the end of a weld connecting a stiffener, diaphragm, etc. to a girder web in a region of combined bending and shear.	E	This classification includes all attachments to girder webs.	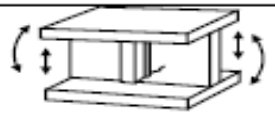
6.3 Parent metal adjacent to welded shear connectors.			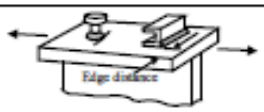
(a) Edge distance ≥ 10mm.	F		
(b) Edge distance < 10mm (see Type 4.2).	G		
6.4 Parent metal at the end of a partial length welded cover plate, regardless of whether the plate has square or tapered ends and whether or not there are welds across the ends.	G	This Class includes cover plates which are wider than the flange. However, such a detail is not recommended because it will almost inevitably result in undercutting of the flange edge where the transverse weld crosses it, as well as involving a longitudinal weld terminating on the flange edge and causing a high stress concentration.	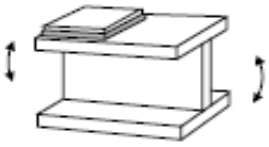
6.5 Parent metal adjacent to the ends of discontinuous welds, e.g. intermittent web/flange welds, tack welds unless subsequently buried in continuous runs.	E	This also includes tack welds which are not subsequently buried in a continuous weld. This may be particularly relevant in tack welded backing strips. Note that the existence of the cope hole is allowed for in the joint classification	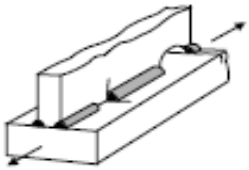
Ditto. Adjacent to cope holes.	F	It should not be regarded as an additional stress concentration.	

Appendix B

Stiffness Calculation

The stiffness of the specimen is performed using the recorded data of force and displacement. The stiffness curve is determined according to the definition as the load divided by the displacement.

$Stiffness = Force/Displacement$ [kips/in]

The initial stiffness of the welded cruciform is considered to be an average stiffness of first 1000 cycles, to be consistent. Then, the cycle count where the initial average stiffness of 1000 cycles is reduced by 50% is the fatigue life of the specimen.

Vita

The author was born in Kathmandu, Nepal. She received her Bachelor's degree in Naval Architecture and Marine Engineering from the University of New Orleans in 2011. She continued with the graduate study under the same concentration after her graduation. She will obtain her Master's degree in Naval Architecture & Marine Engineering in May 2013. She has worked for Dr. Pingsha Dong as a graduate research assistant in the School of Naval Architecture & Marine Engineering for two years. She interned previously at American Bureau of Shipping, Houston, TX.